A STUDY OF THE EFFECTS OF FEED DISPLACEMENT AND REFLECTOR DEFORMATION ON THE PERFORMANCE OF PARABOLIC REFLECTOR ANTENNAS

A Thesis Submitted
In Partial Fulfilment of the Requirements
for the Degree of
MASTER OF TECHNOLOGY

By
FLT. LT. J. R. SWARNAKAR

to the

DEPARTMENT OF ELECTRICAL ENGINEERING
INDIAN INSTITUTE OF TECHNOLOGY KANPUR
AUGUST 1974

CERTIFICATE

This is to certify that the thesis entitled, 'A Study of the Effects of Feed Displacement and Reflector Deformation on the Performance of Parabolic Reflector Antennas' is a record of the work carried out by Flt.Lt. J.R.Swarnakar, under my supervision and that it has not been submitted elsewhere for a degree.

N C Mathur

Dr. N.C. Mathur
Professor
Department of Electrical Engineering
Indian Institute of Technology
Kanpur

Kanpur
Aug, 1974

ACKNOWLEDGEMENTS

'Words but partially convey the feeling and emotions of a man'

Vivekanand.

The above is true of my feeling of indebtedness and gratitude to Dr. N.C. Mathur for his stimulating assistance and expert guidance. So I will not attempt to convey them. I will just say that I sincerely thank him for all the help and encouragement he has given me in the preparation of this thesis.

I also thank Mr. I.J.Bahl for providing valuable assistance in laboratory work. Thanks are also due to the staff of computer center and my colleagues for valuable help for computer work.

I finally thank Mr. K.N.Tewari for his excellent and neat typing.

CONTENTS

		Page
List of Figures		vi
Abstract		viii
CHAPTER I	INTRODUCTION	1
1.1	General	1
1.2	Historical survey of beam steering with fixed parabolic reflectors	1
1.3	Statement of the problem	4
CHAPTER II	PARABOLIC REFLECTOR WITH PYRAMIDAL HORN FEED	9
2.1	Parabolic Reflectors	9
	2.1.1 Geometrical parameters	9
	2.1.2 Aperture distribution	12
2.2	Analytical expression for radiation pattern of paraboloid fed with pyramidal horn	15
2.3	Radiation patterns of horn feed and combined antenna	21
CHAPTER III	EFFECTS OF ABERRATIONS ON LARGE PARABOLIC REFLECTOR ANTENNAS	26
3.1	General	26
3.2	Aberrations effecting parabolic reflectors with horn feed	27
	3.2.1 Linear phase shift	27
	3.2.2 Focus	28
	3.2.3 Coma	29
	3.2.4 Astigmatism	30
3.3	Aberrations not critical with horn feed paraboloids	31
	3.3.1 Spherical	31
	3.3.2 Depolarization	32

3.4	Tolerance in parabolic reflectors	32
	3.4.1 Tolerance in defocusing	33
	3.4.2 Tolerance in astigmatism	34
CHAPTER IV	SIMULATION OF RADIATION PATTERN OF PARABOLIC ANTENNA WITH ABERRATIONS	37
4.1	Analytical expression for radiation pattern and computation with displacement of feed along boresight	37
4.2	Analytical expression for radiation pattern and computation of beam steering with lateral displacement of feed in focal plane	41
4.3	Astigmatism in parabolic antennas	50
	4.3.1 Astigmatism due to imperfection in surface	50
	4.3.2 Astigmatism due to gravitational sag	53
CHAPTER V	MEASUREMENT OF RADIATION PATTERNS	60
5.1	Antenna pattern measurement by ordinary methods	60
5.2	Measurement of antenna radiation patterns of large parabolic fixed dishes	65
	5.2.1 Measurement of radiation pattern with the aid of aircraft	67
	5.2.2 Measurement of radiation pattern with the aid of extraterrestrial sources of radio emission	68
CHAPTER VI	RESULTS AND DISCUSSION	
6.1	Summary of results and discussion	71
	6.1.1 Defocusing	71
	6.1.2 Off-set feed	71
	6.1.3 Astigmatism	74
6.2	Conclusions	74
APPENDIX A		77
REFERENCES		80

LIST OF FIGURES

Fig.No.		Page
1.1	Sectional diagram of parabolic dish	8
2.1	Geometrical parameters for the paraboloidal reflector	10
2.2	Sectional view of paraboloid in XY plane	10
2.3	Pattern of uniformly illuminated rectangular aperture	10
2.4	Paraboloid fed with horn	16
2.5	Horn feed with waveguide to coaxial transition	19
2.6	Pyramidal horn	22
2.7	Pattern of pyramidal horn	22
2.8	Pattern of parabolic dish illuminated by pyramidal horn	24
3.1	Paraboloid with displacement of feed on boresight	35
3.2	Paraboloid with astigmatism	35
4.1	Geometry of paraboloid with axially defocused feed	38
4.2	E-Plane pattern of paraboloid antenna with defocusing	42
4.3	H-Plane pattern of paraboloid antenna with defocusing	43
4.4	Paraboloid with displacement of feed in transverse plane	43
4.5	E-plane pattern of paraboloid antenna with lateral feed displacement	48
4.6	H-plane pattern of paraboloid antenna with lateral feed displacement	49
4.7	Paraboloid with astigmatism due to gravitational sag	54

Fig.No.		Page
4.8	Aperture phase with astigmatism	54
4.9a	E-plane pattern of paraboloid antenna with astigmatism due to gravitational sag	56
4.9b	-do-	57
4.10a	H-plane pattern of paraboloid antenna with astigmatism due to gravitational sag	58
4.10b	-do-	59
5.1	E-plane pattern of paraboloid dish in X band	62
5.2	H-plane pattern of paraboloid dish in X band	63
5.3	Flight pattern for measuring cross-sections of antenna beam	66
5.4	An example of a recording of the draft curve of a source CYGNUS-A through an antenna directional pattern	66

ABSTRACT

The performance of parabolic reflector antennas is very sensitive to the feed position and the reflector surface imperfections. It is possible to obtain a limited amount of beam steering by feed displacement. It is, therefore, of great interest to study the effects of feed displacement and reflector deformation on the radiation patterns of these antennas. The feed displacement is either along the bore-sight or in the transverse plane. Similarly the deviation in reflector surface from the true paraboloidal surface in case of deformation is either due to imperfection in manufacturing the surface or due to change in reflector shape because of gravitational sag.

Effects on the radiation patterns in all these cases have been considered in relation to a 28 ft parabolic reflector dish fed by a pyramidal horn which is being used in a troposcatter link being operated by IIT Kanpur. It is assumed that the magnitude of the effective aperture distribution remain unchanged since the displacement or deviation considered are very small in comparison to reflector parameters. They only cause a change in the phase factor so that the aperture of parabolic dish deviates from an equi-phase surface.

The analytical expressions for computing radiation patterns in E-plane and H-plane for various cases are obtained in convenient integral form. Power patterns for varying displacements of feed and deviation in surface have been plotted for carrying out a critical analysis. As the facilities do not exist for actual measurement of radiation pattern on 28 feet dish, efforts have been made to measure the radiation patterns of a small parabolic dish of 30 cm aperture diameter fed by a E-plane sectorial horn in the laboratory with varying feed displacement. The results have been compared with those obtained by simulation on the computer for the same small dish. A mention has been made of the technique of measuring the radiation patterns of large fixed parabolic reflector antennas by flying an aircraft in the radiation zone. Another technique discussed is the use of radio astronomical sources for antenna pattern measurements.

The curves of radiation patterns reveal that the displacement of feed along boresight causes defocusing of radiation pattern by increasing its half power beamwidth, blending side lobes into main beam and bringing a reduction in field intensity. The displacement of feed in transverse plane causes a tilt in the main beam coupled with reduction in field intensity and increase in beamwidth. The beam tilt provides the possibility of achieving a beam scan, but comatic aberration restricts the range of beam scan by severly degrading the pattern for

displacement of feed larger than one wavelength. The deformation of reflector surface brings the effects of astigmatism in parabolic reflector. Astigmatic aberration, specially due to gravitational sag also causes severe degradation of radiation pattern.

CHAPTER I

INTRODUCTION

1.1 General

It is generally required that the antenna directional patterns in majority of the present day applications of large parabolic reflector antennas should be steerable over a fairly large angle. In normal case, this can be achieved by mechanically steering the reflector structure. With large antennas along with the associated back-up structure, the steering mechanism may itself become a major problem. In parabolic reflector antennas, steering of beam in a small range can be achieved by displacing the feed in the focal plane without resorting to the costly steerable mechanism for the whole antenna system. This displacement of feed in the transverse plane can cause other aberrations, chiefly, defocussing, coma and astigmatism.

1.2 Historical Survey of Beam Steering with Fixed Parabolic Reflectors

The study of radiation patterns of parabolic reflectors illuminated by a source at its focal-point and achieving beam steering by mechanically moving the feed structures have been done extensively. In 1946, Hildebrand and Mauchley first studied and presented the results for an off-set dipole feed in the integral form. Kelleher and Coleman reduced this problem to one space dimension in 1952 and applied to a

Gaussian type aperture field distribution. The analysis was based on current distribution in the aperture plane, neglecting higher order perturbations in the radial variable.

Sandler [16] approached the problem in a similar manner taking into account all phase errors due to an off-axis dipole and tapered amplitude source. He also worked on the problem by scalar diffraction theory and presented the solution in terms of familiar Bessel Functions. Comparing with his experimental results, he found that the two approaches yield similar results only for small values of off-set which provides beam scan of much less than one standard beamwidth (SBW). A standard beamwidth is defined as a half-power beamwidth for an equivalent paraboliid fed by a dipole source located at the focus. At higher values of off-set, the results indicates a rather low order of agreement compared to rigrous theoretical calculations.

In 1965 John Ruze [10] presented his study of beam scanning of fixed paraboloids by lateral feed displacement in transverse plane based on scalar plane wave theory and making use of series expansion of the phase aberration function. He compared the effects of aberration due to lateral feed displacement with classical study of aberrations in optical system. The aberration in optics have been extensively investigated by Nijboer and Nienhuis, Kingslake and others, and excellently presented in the text by Born and Wolf. Ruze explained, how these results of optical papers are not immediately applicable to antenna theory. He assumed that magnitude of aperture illumination remains unchanged by slight displacement of feed and

only phase of aperture field varies because of phase error factors. This provide beam scanning accompanied by degradation of pattern due to defocus, coma and astigmatism. He found that the range of scan is limited by the increasing coma.

In 1969, T. Takeshima [19] presented his approach to the problem also by displacing the feed in the transverse plane, but by progressively defocusing the feed to achieve beam scanning in excess of the angle by which reflector is steered from the boresight. Therefore, his approach had the distinct disadvantage of needing a steering mechanism for reflector structure, though in a very small range. He achieved a beam scanning of $\pm 15^{\circ}$, approximately double of reflector tilt angle without much degradation of radiation patterns, in the vertical and horizontal plane. The advantage of his approach is that it needed no r.f. rotary joint.

Another team to work on beam steering with large fixed paraboloids is of A.W.Rudge and M.T.Withers [15]. It has been shown that the Fourier transform type relationship which exists between the aperture field distribution and the focal plane field distribution occurs not only for waves incident along the boresight of the parabola, but also along a pre-determinable locus for waves ariving at an angle. Therefore, in their approach, the location of the feed is not restricted to the focal plane, and the signal processing employed is that of a spatial Fourier transformation of the intercepted electric field. The primary feed is not a single element, but suitably designed and moved on the pre-determined locus. Although, this involves

movement of a complex feed assembly, the problem compares favourably with that involved in moving the massive reflector structure. The advantage of this approach lie in the fact that, with the movement of the feed array along a defined locus, only an adjustment of phase shifter is required to achieve aberration free scanning of beam. It provides a greater angle of scan than comparative systems, and requires no amplitude weighting of the intercepted energy to maintain optimum signal/noise performance of the antenna system.

1.3 Statement of the Problem

In this thesis several problems related to parabolic reflector antennas are considered. The problems have been considered in relation to a 28 feet parabolic reflector antenna used in a troposcatter link being operated by I.I.T. Kanpur. The details of this antenna are shown in Figure 1.1. The following problems have been studied.

(a) The beam scanning in fixed parabolic reflector antenna fed by a pyramidal horn by displacement of feed in the transverse plane.

(b) The effects of displacing the feed along the boresight on radiation pattern of paraboloid system.

(c) The effects of astigmatism on large parabolic reflectors.

To study the effects of defocusing, lateral feed displacement and astigmatism in the paraboloid antenna system with horn feed, Berkowitz's [3] analysis will be used. The aperture illimination in the vertical and horizontal plane of

the horn feed and of the parabolic reflector antenna will be obtained first. The radiation patterns of horn feed and combined antenna system will then be obtained by numerically computing the integrals.

Throughout the analysis, it will be assumed that the magnitude of the aperture illumination remains unchanged, as the displacement of feed considered is much less compared to the system parameters, and feed is always pointing at the vertex. The feed displacement only causes a phase variation of this illumination in the aperture plane, so that the aperture of the dish is no longer an equiphase surface. Depending upon the extent of phase error, the radiation pattern will change.

In case of defocusing, the phase error factor is of the second order, and it causes symmetrical deformation of radiation pattern. To study this, the feed will be simulated to move on boresight, towards the reflector and away from the reflector from the focus. The change in the phase factor at various points on the aperture plane for each displacement will be computed while computing the integrals by Simpson rule to obtaine radiation patterns of antenna system in the E-plane and H-plane.

To study effects of lateral feed displacement and to find the range of scan of beam by this feed displacement in transverse plane, the analysis presented by Ruze [10] will be followed. The analysis given by Takeshima considers limited steering of main reflection structure and that given by Rudge and

Withere considers a special feed design. So both these later analyses cannot be used in the present experimental link which has a fixed reflector with a single horn feed. The analytical solution by Ruze is presented in integral form having familiar Bessel function as one of the variable. The Bessel function term comprises of linear phase error term and cubic phase error term. The linear phase error factor will provide the beam shift, whereas cubic phase error term will give coma effects on the radiation pattern. These phase error factors will be computed at various point on the aperture plane, then the Bessel's function will be evaluated and along with this integral will be computed again by using Simpson rule for each value of feed displacement. The main beam tilt will increase with progressive increase in the feed displacement. The results show how much of beam scan is possible without much degradation of radiation pattern.

Astigmatism in paraboloc reflector arising from imperfactions in the reflector surface and change in reflector shape due to gravitational sag will be investigated. Cogdell's [5] and Slater's [16] approach will be followed to obtain the phase error factor which best fits the experimental results. Simpson rule will be used again to compute final integrals to obtain the radiation patterns in vertical and horizontal plane of the system.

The effects of these aberrations will be simulated on a small parabolic reflector with aperture diameter of 30 cms, and

f/D ratio of $\frac{1}{3}$, operating at 10 GHz. The results will be compared by practically measuring the radiation patterns in the laboratory. We will also consider, how antenna patterns can be measured practically for large fixed dishes by radio astronomical method and by detecting the field by actually flying an aircraft in the radiation zone.

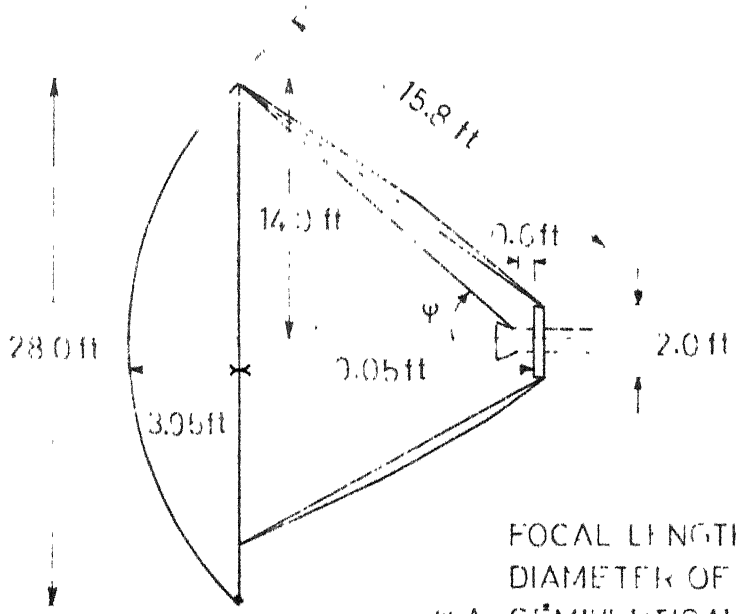

FOCAL LENGTH = 12.4 ft
DIAMETER OF DISH = 28 ft
Ψ ≙ SEMIVERTICAL ANGLE = 58.0 DEG.
f/D = 0.443

FIG. 1.1 SECTIONAL DIAGRAM OF PARABOLIC DISH

CHAPTER II

PARABOLIC REFLECTOR WITH PYRAMIDIAL HORN FEED

2.1 Parabolic Reflectors

2.1.1 Geometrical parameters [11,21]

A paraboloid symmetrical with respect to the x-axis, with its vertex at the origin, is shown in Figure 2.1. This surface possesses several remarkable properties. To discuss them, it is convenient to use several different coordinate systems simultaneously. These coordinate systems are also defined in Figure 2.1. The equation of paraboloid surface in these coordinates is given by

$$y^2 + z^2 = 4 f x \tag{2.1}$$

$$r^2 = 4f x \tag{2.2}$$

$$= \frac{2f}{1 + \cos\psi} = f \sec^2 \left(\frac{\psi}{2}\right) \tag{2.3}$$

where f = OF, is the focal length. To discuss the final antenna pattern, we also use spherical coordinate system with origin at focus and polar axis in positive x-direction. These coordinate are (R, θ, φ), with θ the polar angle and φ the azimuth angle. A section of the paraboloid in Z = 0 plane is shown in Figure 2.2.

The length of the ray from focus to the paraboloid is given as

$$\rho_1 = [(f-x_1)^2 + y_1^2]^{\frac{1}{2}} = [f^2 - 2f\, x_1 + x_1^2 + 4\, f\, x_1]^{\frac{1}{2}} = f + x_1 \tag{2.4}$$

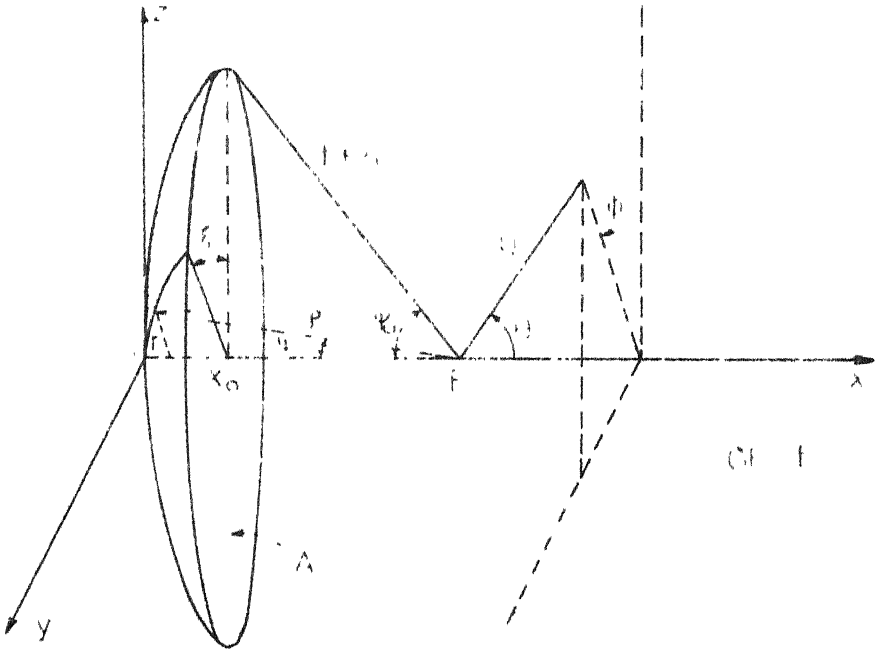

FIG. 2.1 GEOMETRICAL PARAMETERS FOR THE PARABOLOIDAL REFLECTOR.

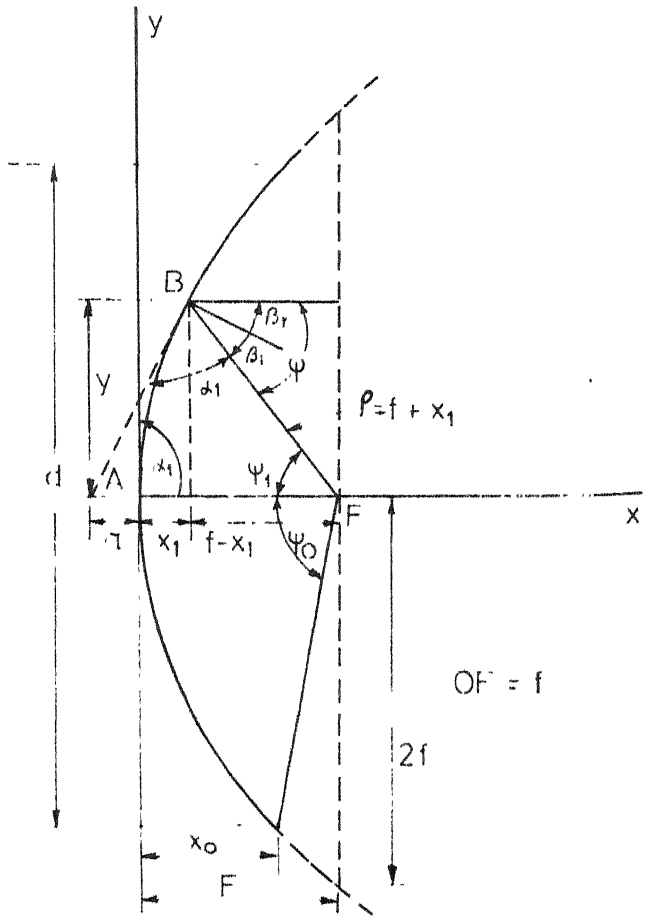

FIG. 2.2 SECTIONAL VIEW OF PARABOLOID IN x y PLANE

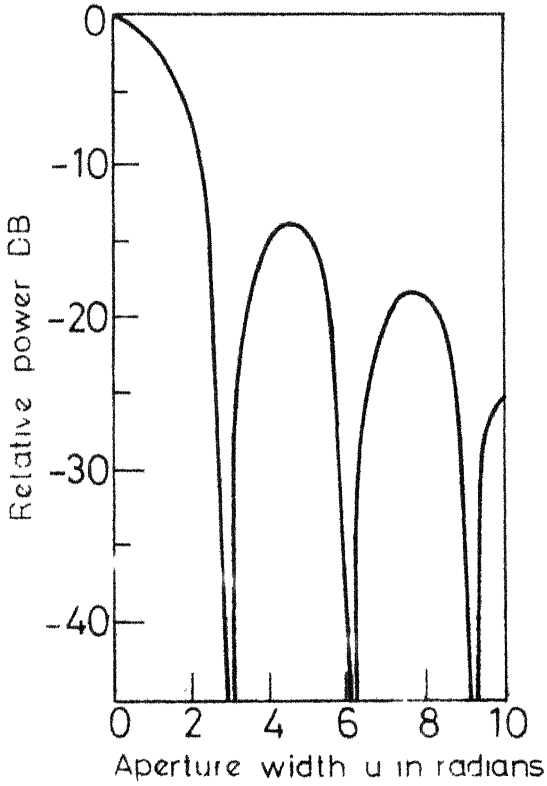

FIG. 2.3 PATTERN OF UNIFORMLY ILLUMINATED

With the help of Eq.(2.1), it can be established that distance from the vertex to the point of intersection between x-axis and tangent at the point of reflection is equal to x, coordinate of the point on paraboloid surface. This characteristic establishes the triangle A B F as an isosceles triangle, which gives

$$\beta_i = \frac{\pi}{2} - \alpha_1 = \tfrac{1}{2}(\pi - 2\alpha_1) = \frac{\psi_1}{2} \qquad (2.5)$$

From Snell's law, the angle of reflection is equal to angle of incidence, therefore the angle between incident ray and reflected ray is equal to angle between incident ray and x-axis. This makes the outgoing ray parallel to the x-axis. The length of this ray from focal point to the reflector and back to the line x = f is

$$r_1 = \rho_1 + (f - x_1) = 2f \qquad (2.6)$$

The shape of the reflector is also specified by angular aperture ψ, the angle between the x-axis and the ray to the reflector. This angle is given by the relation

$$\tan \psi_1 = y_1/(f - x_1) \qquad (2.7)$$

The relation between angular aperture and the f/D radio at edge of dish is given by

$$\sin \psi_o = \tfrac{1}{2}\left(\frac{D/f}{1+D^2/16\ f^2}\right) \qquad (2.8)$$

and

$$\tan \psi_o = \tfrac{1}{2}\left(\frac{D/f}{1-D^2/16\ f^2}\right) \qquad (2.9)$$

The geometrical relationship obtained above are useful for describing the performance of a paraboloid illuminated by a point source at the focus. If the source is not isotropic and the antenna primary feed has some arbitrary distribution, it is

necessary to know the current distribution on the reflector or the fields in the secondary aperture to determine the antenna performance.

2.1.2 Aperture Distribution [6, 21]

The aperture field distribution is of great theoretical and practical interest because it effects the spatial distribution of radiated energy. For a narrow beam antenna, the amplitude distribution f(v) over the aperture controls the main beam shape and width, the sidelobe level, and the side lobe envelope. The electric field for a constant phase aperture, with exp(-jkr)/kr and other nonpertinent factor deleted, in normalized form can be given by the following equations [see Wolff 21, pp. 119-127]

$$F(u) = \frac{L}{2} \int_{-1}^{1} f(v)\, e^{juv}\, dv \qquad (2.10)$$

where

$$u = \frac{\pi L}{\lambda} \sin\theta = \frac{KL}{2} \sin\theta \qquad (2.11a)$$

and

$$v = \frac{2x}{L} \qquad (2.11b)$$

The x variable is the distance measured along the line source from the centre, the source length is L and angle θ is measured from broad side. The far field pattern is the magnitude F(u) . However, when f(v) is an even function, the integral of Eq.(2.10) is real and the pattern is simple F(u).

We will discuss the two distributions: Uniform and Cosine, which fulfills our requirements.

(a) Uniform Line Source:

For a uniformly illuminated aperture, the electric field is constant in amplitude and so substituting $f(v) = 1$ in Eq.(2.10) yields

$$F(u) = \frac{\sin u}{u} \tag{2.12}$$

This is familiar sinc function and is plotted in Figure 2.3. As seen from Figure 2.3, the first side lobe occurs at $u \approx 3\pi/2$ at an amplitude of (-13.2 db). Substituting value of u from Eq. (2.11a), the nulls in this pattern occur approximately at points

$$\sin\left(\frac{\pi L}{\lambda} \sin \theta_n\right) = 0 \tag{2.13}$$

or

$$\frac{\pi L}{\lambda} \sin \theta_n = n\pi \tag{2.14}$$

For relatively large aperture, the first nulls occur at $\theta_1 = \lambda/L$, and the mainbeam-width between the nulls is $BW = 2\lambda/L$. We also see that the half power beamwidth occurs approximately at $u \approx 1.39$, or in the space variable

$$BW_3 = \left(2 \text{ arc sin } \frac{1.39\lambda}{L}\right) \simeq \frac{0.88\lambda}{L} \tag{2.15}$$

In this case the side lobe envelope decay is not constant and the rate of decrease depends on the source length L. From Eq. (2.15) we observe that longer line source will produce narrow beam as the beamwidth is inversely proportional to the aper-

(b) Cosine Distributions:

Another aperture illumination commonly used is the cosine type taper for which the cosine function may be raised for some power. A particular advantage of this general cosine with power n function is that both the space factor integral and the directivity integrals can be obtained in closed form. All such distributions are zero at the line end i.e., there is no pedestal. The first value of n is of interest in practice. However, parameters for higher values can also be found. Substituting $f(v)=\cos \frac{\pi v}{2}$ in Eq.(2.10) yields

$$F(u) = \frac{L}{2} \int_{-1}^{1} \cos \frac{\pi v}{2} e^{juv} dv \qquad (2.16)$$

Solving, we get,

$$F(u) = \frac{L}{\pi} \left[\frac{\cos u}{1 - 4\cdot(\frac{u}{\pi})^2} \right] \qquad (2.17)$$

The first null in this pattern occurs at $u = 3\pi/2$, so that the main beamwidth between nulls is $BW = 3\lambda/L$. Similarly, the half power point occurs at $u = 1.9$, so that the half power beamwidth is

$$BW_3 = 1.2 \frac{\lambda}{L} \qquad (2.18)$$

Also the first side lobe occurs at $u = 2\pi$, with an amplitude of -23.5 db. Parameters for general cosine distributio are given in Table 2.1 where directivity has been normalized by the uniform line source value G_o.

Table 2.1: $\cos^n \frac{\pi v}{2}$ distribution.

n	Side lobe ratio (db)	Beamwidth (rad)	G/G_o
0	13.2	$0.88\lambda/L$	1.00
1	23.0	$1.20\lambda/L$	0.81
2	32.0	$1.45\ \lambda/L$	0.67
3	40.0	$1.66\ \lambda/L$	0.58

2.2 Analytical Expression for Radiation Pattern of Parabolic Reflector Fed with Pyramidal Horn [3,21]

Pyramidal horn feed is the primary source of the parabolic reflector antenna. The radiation pattern of the horn as an isolated unit is known as the primary pattern of the antenna system. The overall pattern of the antenna is called the secondary pattern. In antenna design, one of the major problem is to establish the relationship between the primary and secondary patterns of the antenna. A paraboloid fed with horn is shown in Figure 2.4, where for convenience the paraboloid is cut to occupy a rectangular aperture with sides A and B in the y and z directions, respectively. The horn is fed by a rectangular waveguide which is excited only in the dominant mode TE_{10}. This will give a uniform field in the E-plane and a tapered field in the H-plane.

We will follow the approach by Berkowitz [3] to obtain the analytical expression for radiation pattern of paraboloid system.

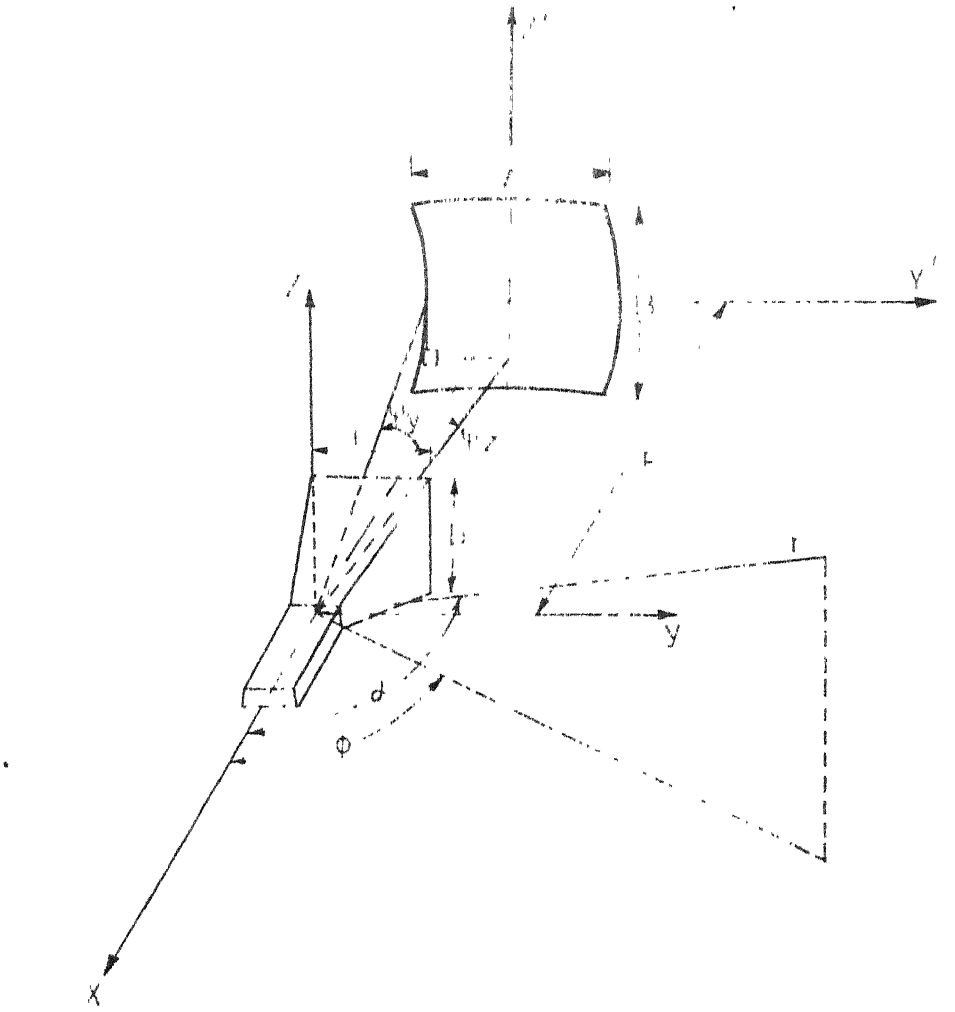

FIG. 2.4 PARABOLOID FED WITH HORN.

From Eq.(2.12), for a uniform field, the E-plane pattern of the horn feed for a horn height b is,

$$f_E = \frac{\sin\left[\frac{kb}{2}\sin\psi_z\right]}{\frac{kb}{2}\sin\psi_z} = \frac{\sin U_E}{U_E} \qquad (2.19)$$

where

$$U_E = \frac{kb}{2}\sin\psi_z \qquad (2.20)$$

In the H-plane, the field is tapered such that at the edge of the horn magnitude of field distribution is zero. A cosine illumination is best suited for such field distribution. Assuming a first order cosine distribution, from Eq.(2.17), the H-plane pattern of the horn feed is

$$f_H = \frac{\cos U_H}{1-4\left(\frac{U_H}{\pi}\right)^2} \qquad (2.21)$$

where

$$U_H = \frac{\pi a}{\lambda}\sin\psi_y \qquad (2.22)$$

The half angle included by the reflector is given as

$$\psi_z = \tan^{-1}\frac{B/2}{f-x_o} \qquad (2.23a)$$

and

$$\psi_y = \tan^{-1}\frac{A/2}{f-x_o} \qquad (2.23b)$$

where, x_o is the distance from vertex to aperture plane and f is the focal length of the paraboloid. As the paraboloid is

symmetrical with respect to x-axis, the aperture diameter D is equal to A as well as B. This gives

$$\sin\psi_z = \sin\left[\tan^{-1}\frac{D/2}{f-x_o}\right] \tag{2.24a}$$

and

$$\sin\psi_y = \sin\left[\tan^{-1}\frac{D/2}{f-x_o}\right] \tag{2.24b}$$

so that the E-plane and H-plane illumination at the edge of the dish is given by

$$f_E(D/2) = \frac{\sin\left[\frac{\pi b}{\lambda}\sin\left(\tan^{-1}\frac{D/2}{f-x_o}\right)\right]}{\frac{\pi b}{\lambda}\sin\left(\tan^{-1}\frac{D/2}{f-x_o}\right)} \tag{2.25}$$

and

$$f_H(D/2) = \frac{\cos\left[\frac{\pi a}{\lambda}\sin\left(\tan^{-1}\frac{D/2}{f-x_o}\right)\right]}{1-4\left[\frac{a}{\lambda}\sin\left(\tan^{-1}\frac{D/2}{f-x_o}\right)\right]} \tag{2.26}$$

Therefore, illumination of the dish at any point in E-plane and H plane is given by,

$$f_E(z) = \frac{\sin\left[\frac{\pi b}{\lambda}\sin\left(\tan^{-1}\frac{z}{f-x_o}\right)\right]}{\frac{\pi b}{\lambda}\sin\left(\tan^{-1}\frac{z}{f-x_o}\right)} \tag{2.27}$$

and

$$f_H(y) = \frac{\cos\left[\frac{\pi a}{\lambda}\sin\left(\tan^{-1}\frac{y}{f-x_o}\right)\right]}{1-4\left[\frac{a}{\lambda}\sin\left(\tan^{-1}\frac{y}{f-x_o}\right)\right]} \tag{2.28}$$

The fields from the dish for secondary patterns are Fourier transform of the distribution of the fields at its aperture,

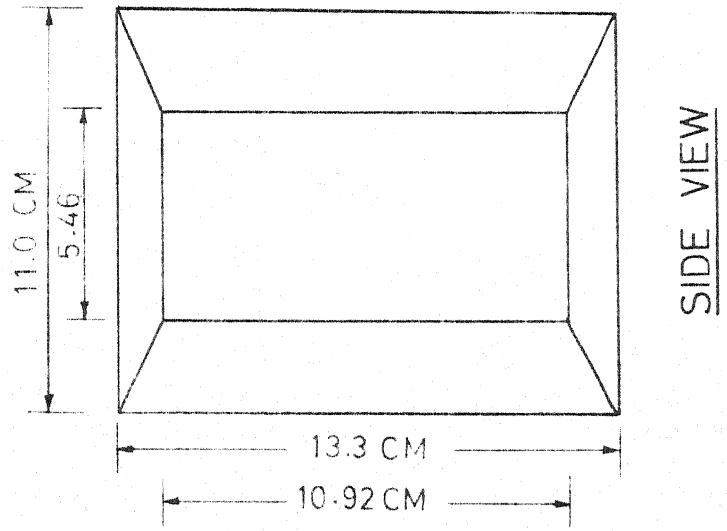

NOTE : DIMENSIONS MENTIONED ARE ALL INSIDE DIMENSIONS

ACCURACY ± 0.5 CM (INSIZE DIMENSIONS)
WALL THICKNESS 2.0 MM
MATERIAL BRASS
ALL DIMENSIONS ARE IN CMS

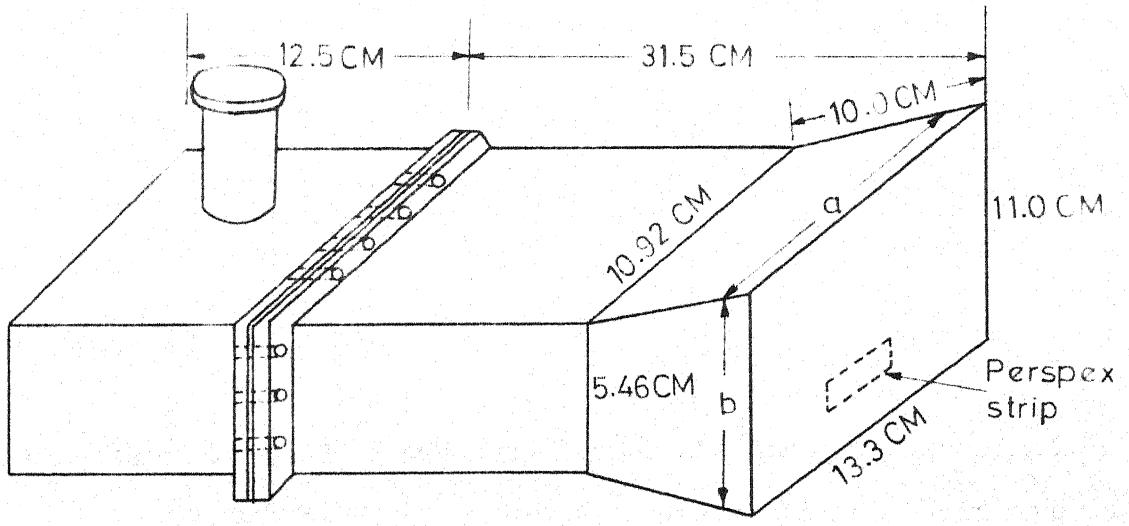

FIG. 2.5 HORN FEED WITH WAVEGUIDE TO COAXIAL TRANSITION.

NOTE :- ALL DIMENSIONS ARE INTERNAL DIMENSIONS.

therefore,

$$E_E = \int_{-\infty}^{+\infty} f_E(z)\, e^{jkz\sin\alpha}\, dz \qquad (2.29)$$

and

$$E_H = \int_{-\infty}^{+\infty} f_H(y)\, e^{jky\sin\alpha}\, dy \qquad (2.30)$$

But our reflector aperture diameter is D. Measuring from its centre, the limits for integration is to be changed to -D/2 to +D/2. Changing the limits, we get

$$E_E = \int_{-D/2}^{+D/2} f_E(z)\, e^{jkz\sin\alpha}\, dz \qquad (2.31)$$

and

$$E_H = \int_{-D/2}^{+D/2} f_H(y)\, e^{jky\sin\alpha}\, dy \qquad (2.32)$$

The power relation in the E and H-plane is given by,

$$E_E^2 = E_{ER}^{\ 2} + E_{Ei}^{\ 2} \qquad (2.33)$$

$$\text{and} \quad E_H^2 = E_{HR}^{\ 2} + E_{Hi}^{\ 2} \qquad (2.34)$$

where, R denotes for real terms and i denotes imaginary terms. The terms of Eq.(2.33) and Eq.(2.34) in computational form are given as

$$E_{ER} = \int_{-D/2}^{+D/2} f_E(z)\, \cos(kz\sin\alpha)dz \qquad (2.35a)$$

$$E_{Ei} = \int_{-D/2}^{D/2} f_E(z) \sin(kz\sin\alpha)\, dz \qquad (2.35b)$$

$$E_{HR} = \int_{-D/2}^{D/2} f_H(y) \cos(ky\sin\alpha)\, dy \qquad (2.35c)$$

and

$$E_{Hi} = \int_{-D/2}^{D/2} f_H(y) \sin(ky\sin\alpha)\, dy \qquad (2.35d)$$

2.3 Computation of Radiation Patterns of Horn Feed and Combined Antenna System

Dimensions for pyramidal horn feed are shown in Figures 2.5 and 2.6. These dimensions are -

E-plane aperture (b)	= 11.0 cm
H-plane aperture (a)	= 13.3 cm
Length of Horn L	= 10.0 cm
Plane length in E-plane ℓ_E	= 19.9 cm
Plane length in H-plane ℓ_H	= 55.9 cm
E-plane flare angle φ_E	= 16.4 deg.
H-plane flare angle φ_H	= 6.8 deg.
Dimension of waveguide	= 10.92x5.46 cms

By using Eqs.(2.19) and (2.21), primary pattern of the above horn in E-plane and H-plane, respectively, were computed. The computer plots of radiation patterns are shown in Figure 2.7. From the curves of Figure 2.7, we have

Half-power beamwidth in E-plane = 2x35 = 70 deg.

Half-power beamwidth in H-plane = 2x39.75 = 79.5 deg.

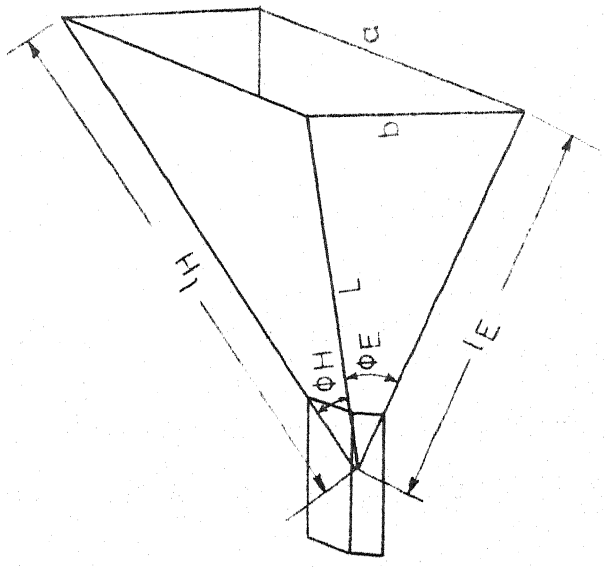

FIG. 2.6 PYRAMIDAL HORN

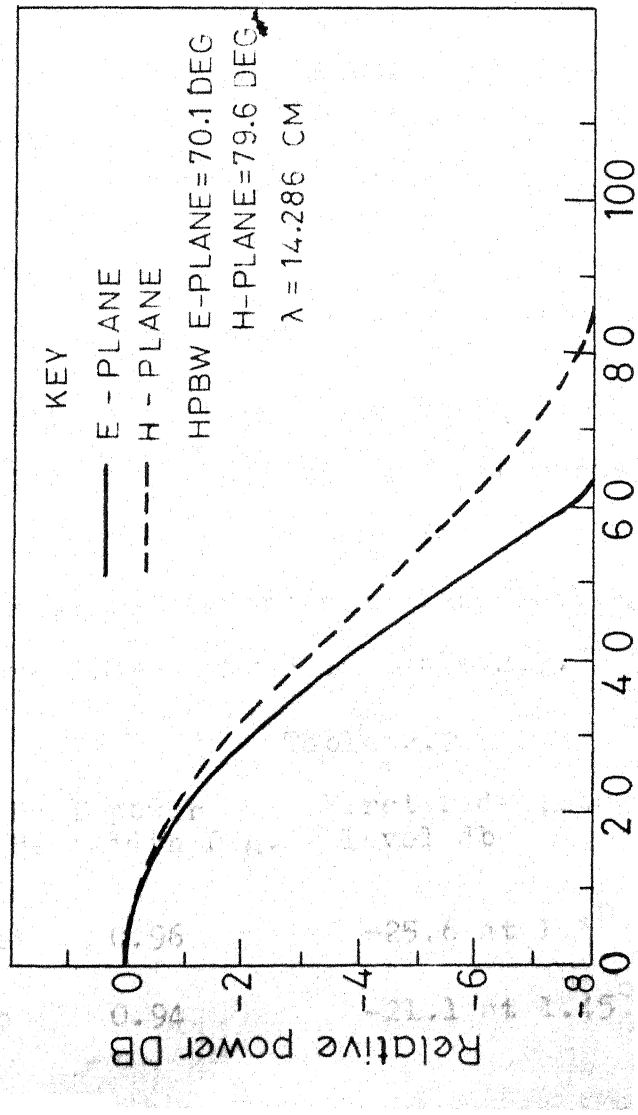

FIG. 2.7 PATTERN OF PYRAMIDAL HORN

Based on practical formula, directivity is given as [4]

$$G = 7.5 \frac{ab}{\lambda^2} = \frac{7.5 \times 13.3 \times 11.0}{(14.286)^2} \qquad (2.36)$$

$$= 5.4 \text{ db}$$

To compute secondary pattern, integrals given by Eqs.(2.35a,b,c,d) are numerically computed using Simpson's rule. Relevant data for parabolic reflectors are shown in Figure 1.1. The parameters given are

Aperture diameter of the dish D = 28.0 ft = 8.55 meters

Focal length f = 12.4 ft = 3.78 meters

Semivertical angle Ψ_o = 58.9 deg.

f/D ratio = 0.443

Frequency of operation = 2.1 GHz

Power radiation pattern based on Eq.(2.33) and Eq.(2.34), and normalized with respect to field at boresight for E-plane and H-plane respectively are computed and plotted in Figure 2.8. Half power beamwidth and side lobe levels obtained from curves from Figure 2.8 are given in Table 2.2.

Table 2.2

	Half power Beamwidth Deg.	First side lobe level db	second side lobe level db
E-plane	0.96	-25.6 at 1.5°	-20.0 at 2.33°
H-plane	0.94	-21.1 at 1.45°	-19.9 at 2.34°

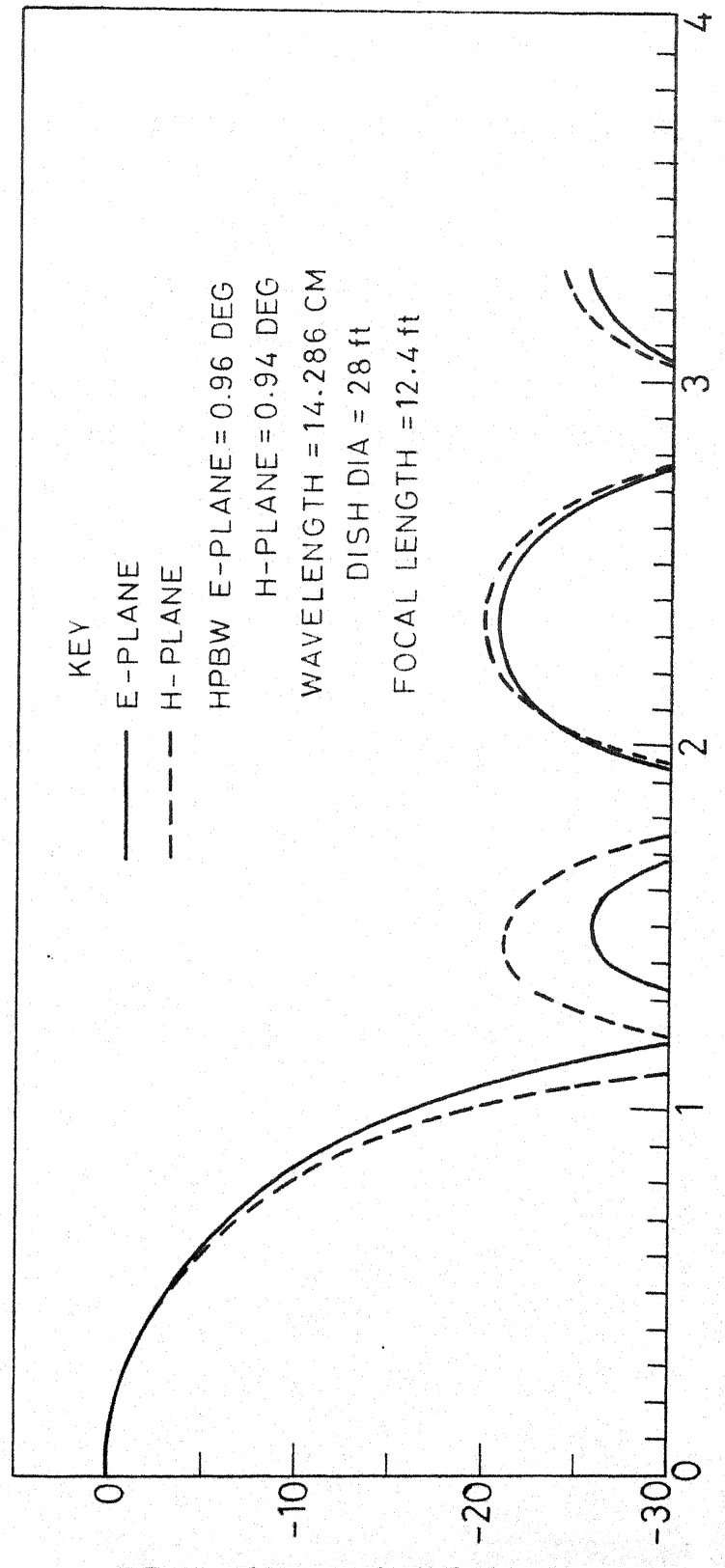

FIG. 2.8 PATTERN OF PARABOLIC DISH ILLUMINATED BY PYRAMIDAL HORN

Gain of the antenna system given by a formula based on experimental results is [9]

$$G = \frac{27,000}{\theta_E \ \theta_H} \qquad (2.37)$$

where θ_E and θ_H are half power beamwidth in Degree. Therefore,

$$G = \frac{27,000}{0.96 \times 0.94} \quad 44.8 \text{ db.}$$

CHAPTER III

EFFECTS OF ABERRATIONS ON LARGE PARABOLIC REFLECTOR ANTENNAS

3.1 General

In large reflecting systems, aberrations are present mainly due to geometry of the system, imperfections in structure and displacement of feed from focus. Effects of these aberrations on radiating aperture depends upon their phase error factors. In case of large parabolic antenna system, the magnitude of aperture illumination remain unchanged whereas non-uniform phase front across the aperture causes undesirable effects upon the radiation pattern. This non-uniform phase front across the aperture can be synthesized in the form of an infinite series as [Hansen 7, pp 139].

$$\beta(a) = 1 + \beta_1 a + \beta_2 a^2 + \beta_3 a^3 + \beta_4 a^4 + \ldots \quad (3.1)$$

where a is the normalized aperture dimension, and β_n is the phase error at the edge of the aperture. β_n will be a function of the reflector f/D ratio and the angle of inclination of the incident wave. The first four terms of infinite series are most important and predominate in the large reflectors. They are commonly termed linear, focus, coma, and spherical aberrations.

Another aberration which is due either to imperfections in the reflecting surface, and/or gravitational sag on the dish, and which can be serious in three dimensional system is astigmatism. It is normally present in all narrow field reflectors.

Lastly, depolarization or the generation of energy in polarization other than the desired polarization can also be considered as an aberration.

3.2 Aberrations Effecting Parabolic Reflector with Horn Feed [7,15]

The aberrations which effects the radiation pattern of parabolic reflector with horn feed are linear, focus, coma and astigmatism. Spherical aberration is more common with spherical antenna and depolarization effects are not present with horn feed.

3.2.1 Linear Phase Shift:

A linear phase shift is not, in reality an aberration, since it does not distort the focal-plane field distribution but merely shift it along the transverse axis. Beam shape is not changed due to this phase error. This linear beam shift due to displacement of feed will be equal to the feed squint where the feed squint is the ratio of feed displacement in focal plane to the focal length of the paraboloid system. However, the shift on transverse axis changes system geometry, which introduces other aberrations, like focus, coma and astigmatism. These aberrations introduces a loss in directivity, changes in side lobe level and degradation of beam. Therefore, a one-to-one correspondence between the angular displacement of the feed and tilt of secondary pattern is not obtained.

The ratio of the angle of shift of main beam to the angle of displaced feed is called the Beam Deviation Factor. Both these angles are measured from the axis of the reflector with the vertex as the origin. The BDF depends upon the aperture illumination and f/D ratio of the reflector system [13]. It has been found from the experimental results that this ratio approaches unity as f/D ratio increases. This in fact is theoretically correct, as coma error is inversely proportional to the square of the system f/D ratio. As coma error reduces, and approach zero, a one-to-one correspondence between the angular displacement and beam deflection should be obtained.

3.2.2 Focus:

The improper placing of the feed in the axial direction is the most common cause of a focus error in a reflecting system. The focus error tends to defocus the field distribution in a symmetrical fashion because it is an even order aberration. The pattern shape is effected, but not the pointing of main lobe. The phase error in the aperture plane illumination in case of a paraboloid system can be approximated by means of the relation [6]

$$\beta(a) = k\,\Delta f(1 - \cos\psi) \qquad (3.2)$$

where, Δf is the displacement of the feed from the focus and ψ is the angle between x-axis and the ray to the reflector.

The effect of this phase error upon the radiation pattern is a reduction in directivity, an increase in beamwidth and a blending of the side lobes into the main beam. From Eq. (3.2),

we observe that the maximum phase error occurs at the edge of the dish, which means that if we have a tapered distribution, the effects of defocusing will be less pronounced as the maximum phase error will occur at the point of minimum amplitude. Wheeler [20] has synthesized an antenna using this property where the pattern broadens with defocusing without changing its shape. It is of great significance in many radar applications.

3.2.3 Coma :

The Abbe' sine condition is not satisfied usually by large reflector systems, that gives rise to coma aberration when feed is displaced in the focal plane. We have observed that a displacement of this kind will shift the main lobe from boresight. This aberration also tends to shift the beam in the opposite direction to that of the linear phase shift along with a loss in directivity. So its effects on radiation pattern are, a squinting of the main beam and an unsymmetrical pattern shape, the sidelobes being higher on the boresight side of the main beam then on the other side. The phase error factor due to coma is function of the f/D ratio of the system and the feed displacement. Coma phase error constitutes the major limitations in paraboloid antenna system to achieve the wide angle beam steering.

The amount of path error due to coma can be calculated with the help of curves illustrated in Hansen [7, pp. 142] which are plots of coma coefficient β_3 versus the tilt in the

main beam, for a f/D ratio of one. The path error at any point on the reflector surface due to coma is given as

$$\text{Path error} = \frac{\beta_3 h^3}{3} \qquad (3.3)$$

where h is distance of the point of measurement on the reflector surface from the centre of the axis. To calculate path error at other f/D ratio, the coma coefficient can be evaluated from the curves by the relation that coma varies inversely as the square of the f/D ratio of the system. As an illustrative example, to calculate path error at edge of a dish with aperture diameter of 28 ft. and f/D ratio of 0.443; to obtain a beam tilt of 5° in a paraboloid antenna system, the path error would be

$$\text{Path error} = \frac{\beta_3 (14)^3}{3(28)^2} \quad ; \quad [\beta_3 = 0.065 \text{ for } f/D = 1]$$

$$= \frac{0.065}{(0.443)^2(28)^2} \cdot \frac{(14)^3}{3} = 0.405 \text{ ft.} = 12.3 \text{ cm.}$$

From the magnitude of this path error, we can predict that the system will give poor pattern performance at x-band, while at lower frequency, say L-band, it might provide satisfactory performance.

3.2.4 Astigmatism:

This aberration arises in any three dimensional system from the fact that the best focus is not same for both the planes. Therefore astigmatism is common in parabolic reflector structure when the feed is displaced in the transverse plane.

Its effects are not apparent until the system performance becomes inadequate due to other aberration, such as coma. This is also a second order phase error.

After adjusting the feed in the lateral plane, such as to give equal side lobe thus eliminating or reducing coma, a position can be found by properly setting the axial position of the feed, which will maximize the gain of the system. With the feed in maximum gain position, the effects on pattern due to remaining second order term is the astigmatism. Thus we conclude that with the feed in optimum position, error upto forth order are eliminated except astigmatism. It is precisely this effect which makes astigmatism so important to recognize, as it cannot be eliminated through focusing.

When astigmatism is due to imperfections in the reflector surface or due to gravitational sag on the heavy structure of reflector, where it gives an effect of squeezing the reflector at opposite edges, it forms the predominant part of phase error factor in degrading the radiation pattern of the system. The effects of this phase error are, reduction in directivity, flattening of main beam, submerging of side lobes and increasing the level of side lobes.

3.3 Aberrations not Critical with Horn Feed Paraboloid

Spherical aberration and aberration due to depolarization comes in this category.

3.3.1 Spherical Aberration:

Spherical aberration is most common in spherical reflecting system. This aberration is of fourth order, therefore, its

effects on radiation pattern are also symmetrical. Actually, the effects of spherical aberration are similar to those of defocusing and so in reality, it is called a higher order focus error.

3.3.2 Depolarization:

The two principal causes of depolarization are the curvature of the reflector surface and the feed itself. When the feed is a short electric dipole positioned properly at focus of a paraboloid, a cross polarized component in the field distribution results in a cross polarized lobe in the 45° plane. This lobe can be higher than the first side lobe of the pattern in the principal polarization. Similar effects takes place in opposite direction when a magnetic dipole is placed at focus of a paraboloid. If a feed consists of a combination of electric and magnetic dipoles oriented at right angle to each other, the result will be cancellation of cross-polarized components. A rectangular horn serves best for this purpose and have very little or no effects due to depolarization.

3.4 Tolerance in Parabolic Reflectors [6] :

Inaccuracy in positioning of the feed at focus and deviation of the reflector surface from actual paraboloid surface are the two main causes to give phase error in the aperture iillumination of a parabolic reflector antenna system. Tolerance in first case can be found out for the extent of shift permissible from focus which will not degrade the radiation pattern abnormally. In second case, manufacturing tolerance

of the reflector surface is of interest as it gives rise to astigmatism in paraboloids. A maximum permissible phase difference of $\pi/2$ in the aperture illumination will be taken as a guide for calculating these tolerances.

3.4.1 Tolerance in Defocusing:

Inaccuracy of this kind is shown in Figure 3.1 where the feed is displaced on boresight by a distance d_1. The phase error introduced can be calculated from simple geometry as [6]

$$\Delta \varphi_1 \simeq \frac{2\pi}{\lambda} [S'M - (s' O + OO')] \qquad (3.4)$$

but

$$S'M \simeq SM - SP = f + x_o - d_1 \cos \psi$$

and

$$S'O = f - d_1$$

$$OO' = x_o$$

$$\Delta \varphi_1 = \frac{2\pi}{\lambda} [d_1 - d_1 \cos\psi]$$

or

$$\Delta \varphi_1 = \frac{2\pi}{\lambda} d_1[1 - \cos\psi] \qquad (3.5)$$

from which we obtain for $\varphi_{1\ max} = \pi/2$.

$$d_{1\ max} = \frac{\lambda}{4(1 - \cos \psi)} \qquad (3.6)$$

$d_{1\ max}$ gives the tolerance of displacement of feed on boresight to give an phase error of $\pi/2$. Radiation pattern for displacement of feed in boresight is computed and plotted in Chapter IV.

3.4.2 Tolerance in astigmatism:

In-accuracy of this kind is expressed in Figure 3.2 where this inaccuracy is expressed as the deviation of reflector surface from the actual parabolic curve. The dotted line corresponds to theoretical contour of the reflector, whereas full curve shows the actual contour of the reflector. Any ray travelling from focus to point M at edge traverses a distance SO" + O" O'. As all rays traverse equal distance in a paraboloid structure, the ray at boresight should also traverse the distance SO" + O" O', but due to actual contour, it traverses a distance SO+OO'. Therefore a path difference of $2d_2$ (where d_2 = OO") occurs between the ray at edge and ray at vertex. This gives a phase error at aperture surface equal to

$$\Delta\varphi_2 = \frac{2\pi}{\lambda} 2d_2 \qquad (3.7)$$

for $\varphi_{2\ max} = \pi/2$, we get tolerance $d_{2\ max}$ as

$$d_{2\ max} = \lambda/8 \qquad (3.8)$$

Considering that the difference from the theoretical curve may have different signs at different points, as is the case explained by Slater [18] it is necessary to take as the manufacturing tolerance on the reflector surface half of that given by Eq.(3.8). Therefore

$$\text{Tolerance } d_2 = \pm \frac{d_{2\ max}}{2} = \pm \frac{\lambda}{16} \qquad (3.9)$$

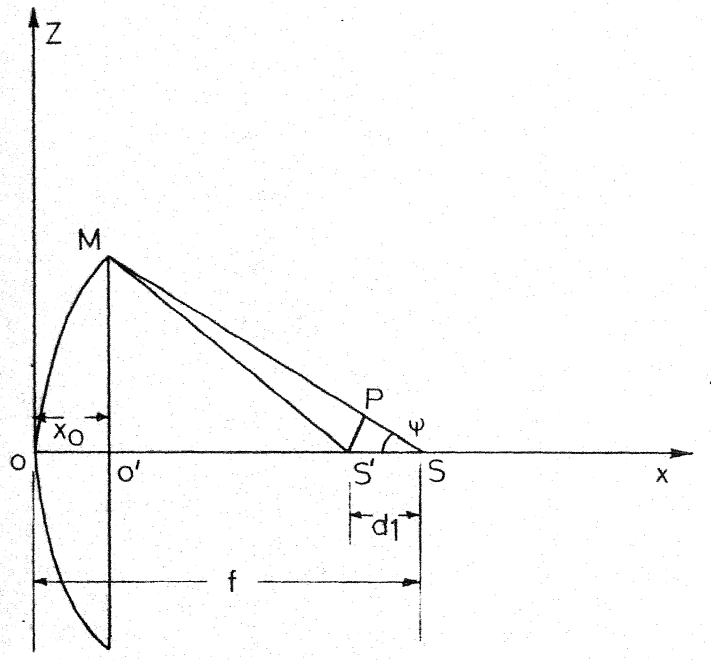

FIG. 3.1 PARABOLOID WITH DISPLACE-
-MENT OF FEED ON BORESIGHT.

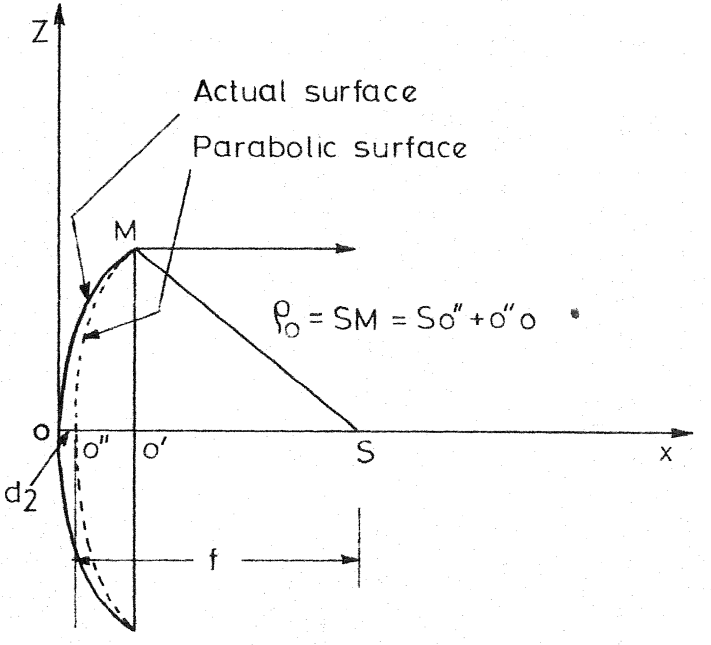

FIG. 3.2 PARABOLOID WITH ASTIGMATISM.

Comparing this with lens antenna, where tolerance is given equal to $\lambda/8(n-1)$ with n as refractive index (1.5 to 1.6), we observe that manufacturing of paraboloid surface requires a greater degree of precision than the lens antennas.

CHAPTER IV

SIMULATION OF RADIATION PATTERNS OF PARABOLOID ANTENNA WITH ABERRATIONS

4.1 Analytical Expression for Radiation Pattern and Computation with Displacement of Feed along boresight

The common cause of defocusing and its general effects on the radiation patterns are already discussed in Section 3.2.2. To obtain an analytical expression to compute secondary pattern of paraboloid, let d be the displacement of feed from focus as shown in Figure 4.1. $\bar{\rho}$ and $\bar{\rho}'$ are the vectors from the feed points to a point on the reflector. The difference in the magnitude of these two vectors is primarily responsible for the antenna's defocusing characteristic. The relationship between ρ and ρ' is given by [8]

$$\rho' = \rho \left\{1 + \left[\frac{d}{\rho}\left(\frac{d}{\rho} - 2\cos\theta'\right)\right]\right\}^{1/2} \qquad (4.1)$$

and the phase error factor will be

$$\Delta\varphi = \frac{2\pi}{\lambda}\left[\rho' - (\rho + d)\right] \qquad (4.2)$$

with the value of ρ' from Eq.(4.1), Eq.(4.2) will make the phase error factor a quadratic error term and solution obtained with this will be termed as complete analysis whereas with simple line of approach, Eq.(4.1) can be approximated as

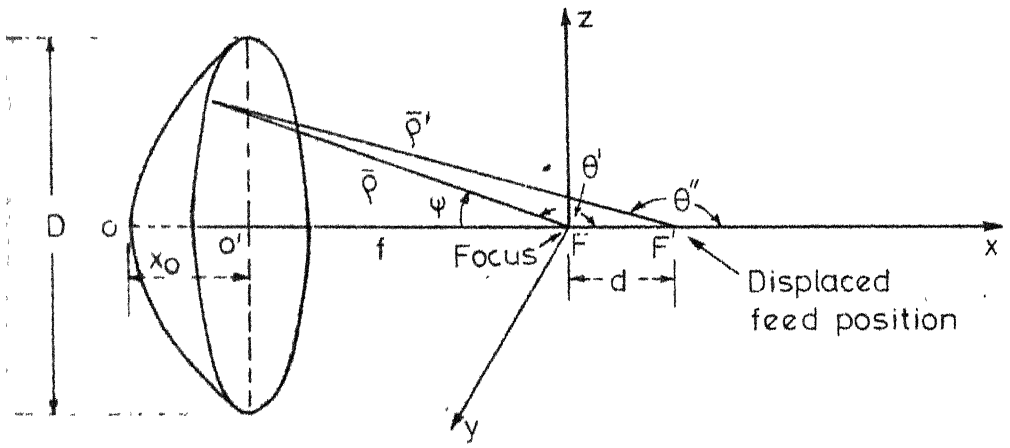

FIG.4.1 GEOMETRY OF PARABOLOID WITH AXIALLY DEFOCUSED FEED.

$$\rho' \simeq \rho \qquad \text{(in amplitude of the aperture illumination)} \qquad (4.3a)$$

$$\rho' \simeq (\rho \pm d \cos\theta') \qquad \text{(in phase relation with positive and negative defocusing)} \qquad (4.3b)$$

With this value of ρ', the phase error factor becomes

$$\Delta\varphi = \frac{2\pi}{\lambda} [\rho \pm d \cos\theta' - \rho \mp d] \qquad (4.4a)$$

$$= \pm \frac{2\pi}{\lambda} d[1 - \cos\psi] \qquad (4.4b)$$

Eq.(4.4b) is similar to that given in Section 3.2.2. This approximation provides linear analysis.

The disadvantage of the complete analysis is that certain closed form expression, which are possible when linear approximations are made, are no longer feasible. However, the complete analysis will indicate the accuracy and range of validity of the linear analysis. Most commonly, linear analysis is used to reduce computation expense. Ingerson and Rush [8] have compared both and found that nulls of linear analysis changes to minima when complete analysis is used. For small displacement of few wavelengths, the results from linear analysis are in close approximation with complete analysis. In our computation, we will follow the linear analysis.

With the phase error factor, the antenna aperture illumination changes from the form given in Sec. 2.2, Eq.(2.27) and (2.28),

$$f'_E(z) = f_E(z)\, e^{\pm jk\Delta\varphi} \tag{4.5a}$$

$$f'_H(y) = f_H(y)\, e^{\pm jk\Delta\varphi} \tag{4.5b}$$

The field in the far zone thus becomes,

$$E'_E = \int_{-D/2}^{D/2} f_E(z)\, e^{jkz\sin\alpha}\, e^{\pm jk\Delta\varphi}\, dz \tag{4.6a}$$

$$E'_H = \int_{-D/2}^{D/2} f_H(y)\, e^{jky\sin\alpha}\, e^{\pm jk\Delta\varphi}\, dy \tag{4.6b}$$

and with similar development, the integrals to plot power pattern will be

$$E'_{ER} = \int_{-D/2}^{D/2} f_E(z)\, \cos[k(z\sin\alpha \pm d(1-\cos\psi))]\, dz \tag{4.7a}$$

$$E'_{Ei} = \int_{-D/2}^{D/2} f_E(z)\, \sin[k(z\sin\alpha \pm d(1-\cos\psi))]\, dz \tag{4.7b}$$

$$E'_{HR} = \int_{-D/2}^{D/2} f_H(y)\, \cos[k(y\sin\alpha \pm d(1-\cos\psi))]\, dy \tag{4.7c}$$

and

$$E'_{Hi} = \int_{-D/2}^{D/2} f_H(y)\, \sin[k(y\sin\alpha \pm d(1-\cos\psi))]\, dy \tag{4.7d}$$

The computation of these integrals are performed for the 28 ft parabolic antenna discussed earlier with the Simpson's rule and power patterns in E-plane and H-plane are plotted in Figure 4.2 and Figure 4.3 respectively for a feed displacement of $\lambda/4$, $\lambda/2$, $3\lambda/4$ and λ on the boresight. As the curves are calculated using linear analysis, they are identical for positive and negative defocusing. Ingerson and Rush have shown (using complete analysis) that there is a slight shift of minima towards boresight with negative defocusing and away from boresights with positive defocusing. The curves of Figure 4.2 and 4.3 are normalized by the total feed power radiated with feed at focus so that spill over is included.

4.2 Analytical Expression for radiation Pattern and Computation of Beam Scanning with Lateral Displacement of Feed Horn

Let the displacement of feed be ϵ as shown in Figure 4.4. With aperture diameter D = 2a, the field at a far point with feed at focus, is given in spherical coordinates as [10]

$$E(\theta, \varphi) = \int_0^{2\pi} \int_0^{a} f(r, \varphi')\, e^{jk(\rho - \bar{\rho}\cdot\bar{R}_o)}\, r\, dr\, d\varphi' \qquad (4.8)$$

where $f(r, \varphi')$ is an effective aperture distribution and all constant factors are suppressed. With displacement of feed, the field at far point changes to,

$$E(\theta, \varphi) = \int_0^{2\pi} \int_0^{a} f(r, \varphi')\, e^{jk(\rho' - \bar{\rho}'\cdot\bar{R}_o)}\, r\, dr\, d\varphi' \qquad (4.9)$$

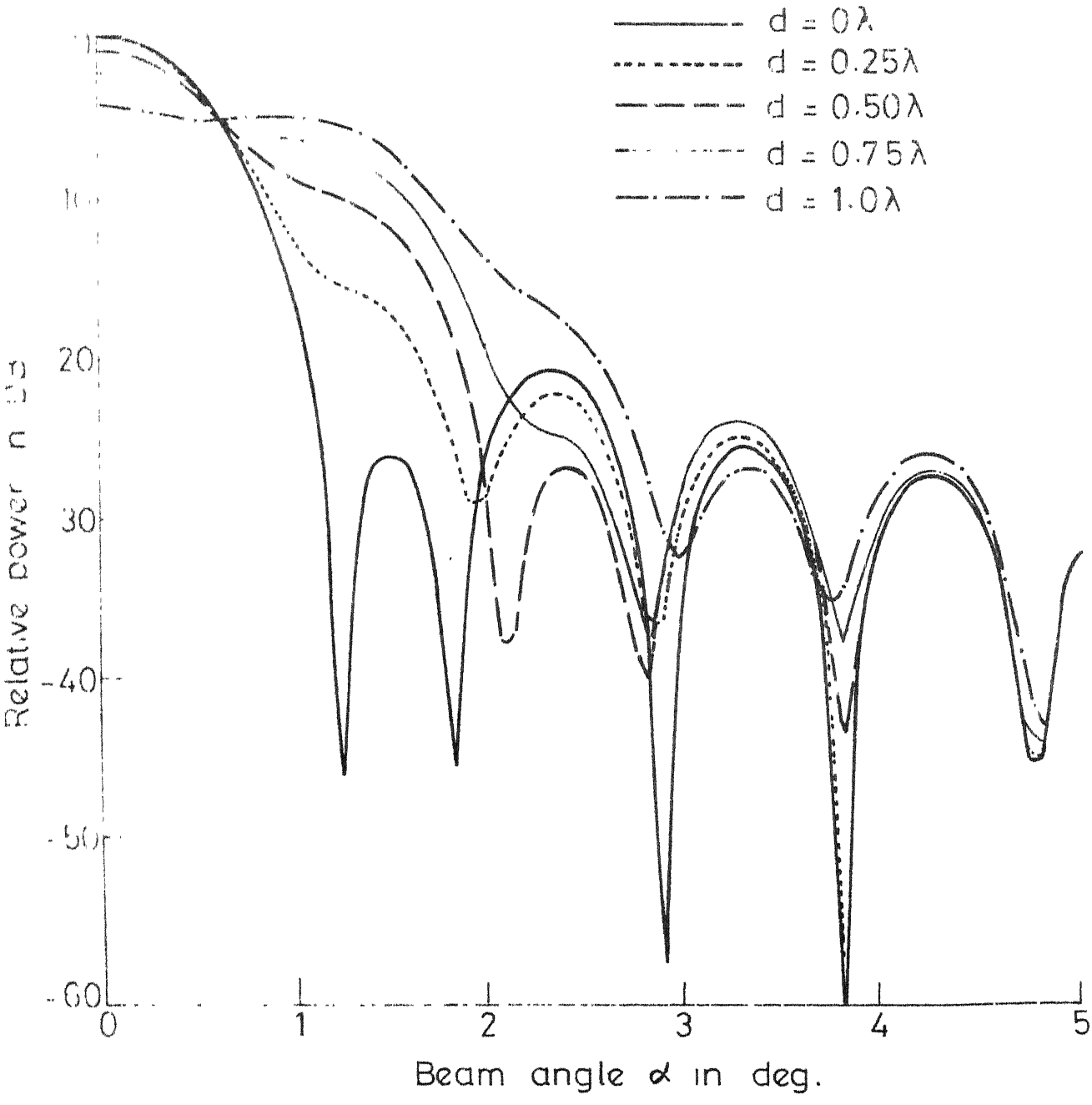

FIG. 4.2 E-PLANE PATTERN OF PARABOLOID FOR DEFOCUSIN

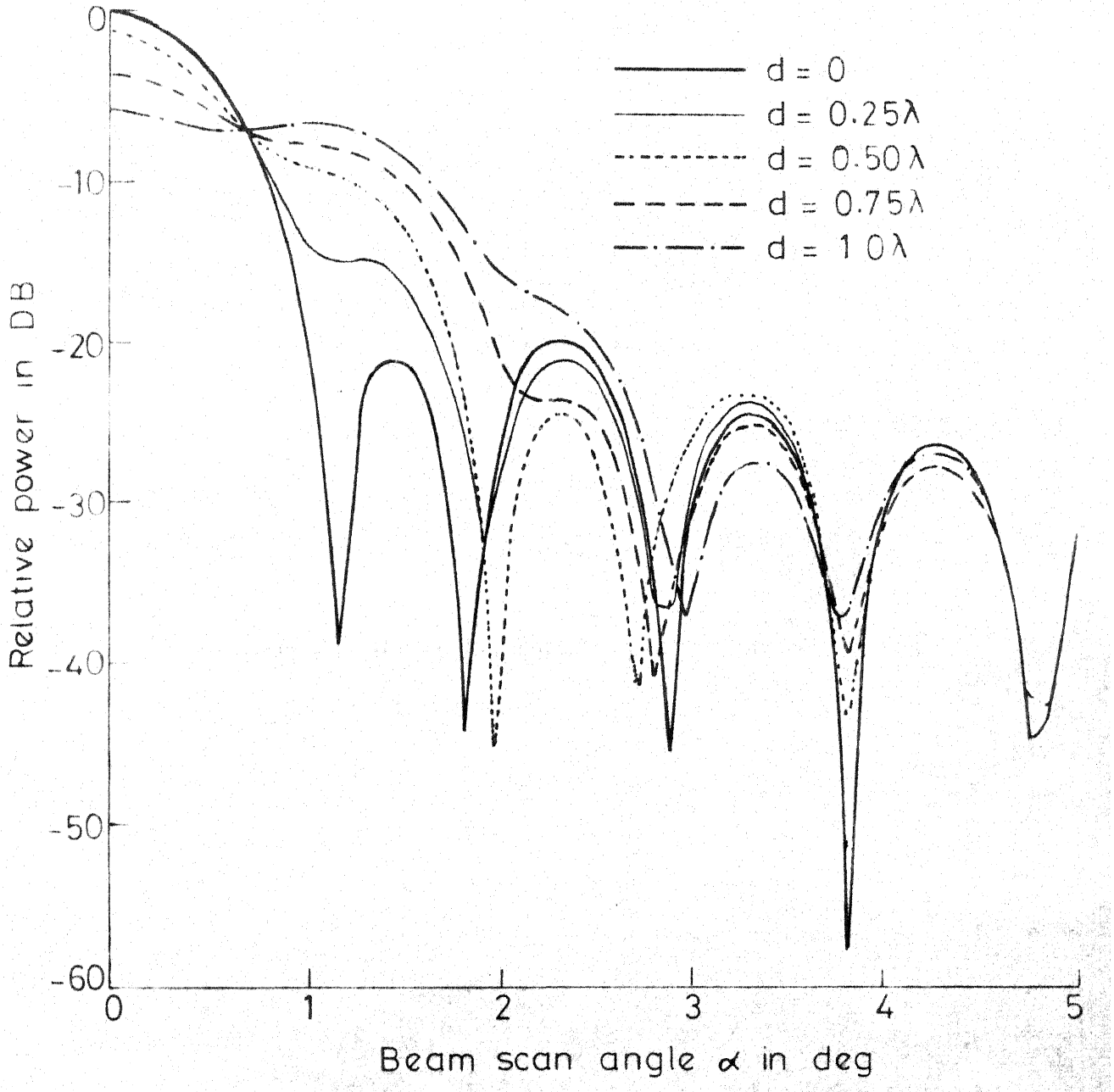

FIG. 4.3 H-PLANE PATTORN OF PARABOLOID ANTENNA WITH DEFOCUSING

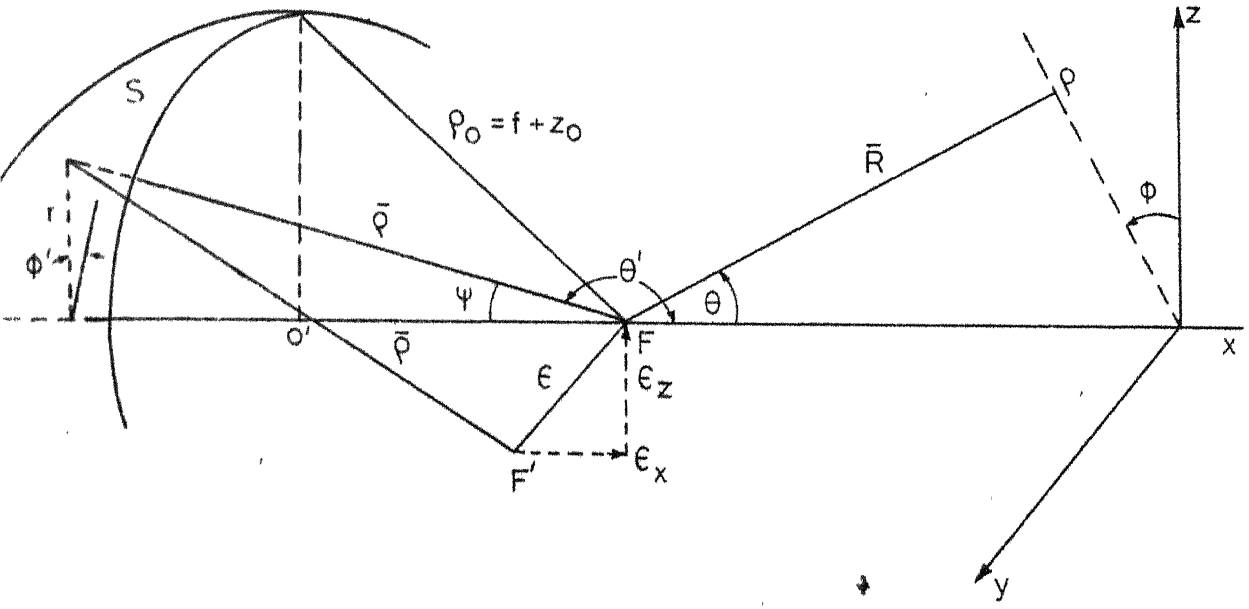

FIG.4.4 PARABOLOID WITH DISPLACEMENT OF FEED IN TRANSVERSE PLANE.

From the Figure 4.4, we have geometric relations

$$\rho = \frac{2f}{1 - \cos\theta'} = \frac{2f}{1 + \cos\psi} = f \sec^2 \frac{\psi}{2} \qquad (4.10a)$$

$$\bar{\rho} = \rho [\cos\theta' \bar{x} + \sin\varphi' \sin\theta' \bar{y} + \cos\varphi' \sin\theta' \bar{z}] \qquad (4.10b)$$

$$\bar{R}_o = [\cos\theta \bar{x} + \sin\varphi \sin\theta \bar{y} + \cos\varphi \sin\theta \bar{z}] \qquad (4.10c)$$

$$\rho' = \rho + \varepsilon_x \bar{x} + \varepsilon_z \bar{z} \qquad (4.10d)$$

$$\rho' = \left[1 + \frac{2\varepsilon_x}{\rho} \cos\theta' + \frac{2\varepsilon_z}{\rho} \cos\varphi' \sin\theta' + \frac{\varepsilon^2}{\rho^2}\right]^{\frac{1}{2}} \qquad (4.10e)$$

Neglecting higher order terms of $\frac{\varepsilon_x}{\rho}$ and $\frac{\varepsilon_z}{\rho}$ as $\frac{\varepsilon_x}{\rho} < \frac{\varepsilon_x}{f} << 1$, the phase factor of Eq.(4.9) is given as

$$\rho' - \bar{\rho}'.\bar{R}_o = [2f - \varepsilon_z \cos\varphi \sin\theta - \varepsilon_x \cos\theta] - [\rho \sin\theta' \sin\theta \cos(\varphi' - \varphi)] + [\varepsilon_z \cos\varphi' \sin\theta'] + [\varepsilon_x \cos\theta' + \frac{\varepsilon_z^2}{2\rho} + \rho \cos\theta'(1 - \cos\theta)] - [(\varepsilon_z^2/2\rho(\cos^2\varphi' \sin^2\theta] \qquad (4.11)$$

In the above equation, first three terms are independent of the integration coordinates and may be taken out of integral and included in constant factor. They represent a phase pattern of the field. As $r = \rho \sin\theta'$, the normal phase factor due to an in phase aperture is given by the next term. The fifth term represents the phase error factor which encompasses linear,

cubic and higher order odd power of integration coordinate. This provides the beam shift and comatic aberration.

The next three terms are proportional to r^2 and higher order even power terms which can be eliminated by refocusing the feed. The last term is the astigmatism. Refocusing condition gives the petzval surface in optics, which is defined as the locus which contains a sharp image when the other aberrations are bent. Setting the field curvature and higher order even power terms to zero, we get locus of feed as

$$\varepsilon_x = \frac{\varepsilon_z^2}{2f} \tag{4.12}$$

Therefore, for sharpest null, the feed locus for small aberration is defined by Eq.(4.12) as another paraboloid of focal length f/2, tangent to the focal plane. With feed in optimum position as discussed in Section ~~x~~3.2.4, and neglecting the astigmatism in comparison to comatic aberration, the magnitude of the far field can be written from Eq.(4.9) as,

$$E(\theta, \varphi) = \int_0^{2\pi} \int_0^{a} f(r,\varphi') \, e^{-jk[r \sin\theta \cos(\varphi'-\varphi) - \varepsilon_z \sin\theta' \cos\varphi']} \, r \, dr \, d\varphi' \tag{4.13}$$

Since

$$\sin\theta' \approx \frac{r}{f}/[1+(\frac{r}{2f})^2] \approx \frac{r}{f}[1 - (\frac{r}{2f})^2 + (\frac{r}{4f})^4 - \ldots] \tag{4.14}$$

The phase error factor may be given as

$$\Delta\varphi = \frac{2\pi}{\lambda}\,\varepsilon_z \sin\theta' \cos\varphi' = \frac{2\pi}{\lambda}\,U_S\, r\left[1-\left(\frac{r}{2f}\right)^2+\left(\frac{r}{4f}\right)^4 - \ldots\right]\cos\varphi' \tag{4.15a}$$

$$= \frac{2\pi}{\lambda}\,U_S r\,\frac{\cos\varphi'}{M(r)} \tag{4.15b}$$

where,

$M(r) = 1 + (r/2f)^2$, and

$U_S = \varepsilon_z/f$ the feed squint.

The first term of Eq.(4.15) is a linear term and provides an undistorted beam shift equal to feed squint. The second term proportional to $U_S r^3 \cos\varphi'$ is, what is known as primary coma and creates beam degradation and a beam shift in the opposite direction, making the beam deviation far from one-to-one correspondence. This ratio has been defined earlier in Section 3.2.1 as beam deviation factor (BDF). The remaining higher order terms are normally neglected. With $u = \sin\theta$, the phase factor term of Eq.(4.13) can be simplified as

$$\text{Phase factor} = Kr\left[U\cos(\varphi' - \varphi) - \frac{U_S \cos\varphi'}{M(r)}\right] = AKr\cos(\varphi'-\alpha) \tag{4.16}$$

where

$$A = U^2 - \frac{2U\,U_S}{M(r)}\cos\varphi + \frac{U_S^2}{M^2(r)} \tag{4.17a}$$

$$\tan\alpha = \frac{U\sin\varphi}{U\cos\varphi - \dfrac{U_S}{M(r)}} \tag{4.17b}$$

and Eq.(4.13) becomes,

$$E(\theta, \varphi) = \int_0^{2\pi} \int_0^{a} f(r, \varphi') \, e^{jkrA\cos(\varphi'-\alpha)} \, r \, dr \, d\varphi' \quad (4.18)$$

For circularly symmetrical illumination functions, the φ' integration can be performed with the result,

$$E(\theta, \varphi) = 2\pi \int_0^{a} f(r) \, J_o(K \, r \, A) \, r \, d \, r \quad (4.19)$$

Eq.(4.19) can be evaluated for specified illumination. For the illumination given in E-plane and H-plane respectively by Eq.(2.27) and Eq.(2.28), Eq.(4.19) yields on normalization and dropping all constants,

$$E_E = \int_0^{1} f_E(z) \, J_o(K \, z \, A) \, z \, d \, z \quad (4.20a)$$

and

$$E_H = \int_0^{1} f_H(y) \, J_o(K \, y \, A) \, y \, dy \quad (4.20b)$$

Power patterns calculated from Eq. (4.20 a and b) are plotted in Figure 4.5 and 4.6 for E and H-plane respectively with different displacement of feed. The computer program is given as Appendix 'A'.

In our analysis, we have neglected the astigmatism in comparison to coma terms. It is of interest to examine the ratio of the total coma aberration with neglected astigmatism, which is given as [10]

$$\frac{\text{Astigmatism}}{\text{Total coma}} = \frac{2 \, U_S \, (f/D)}{[1+(D/4f)^2]^2} \quad (4.21)$$

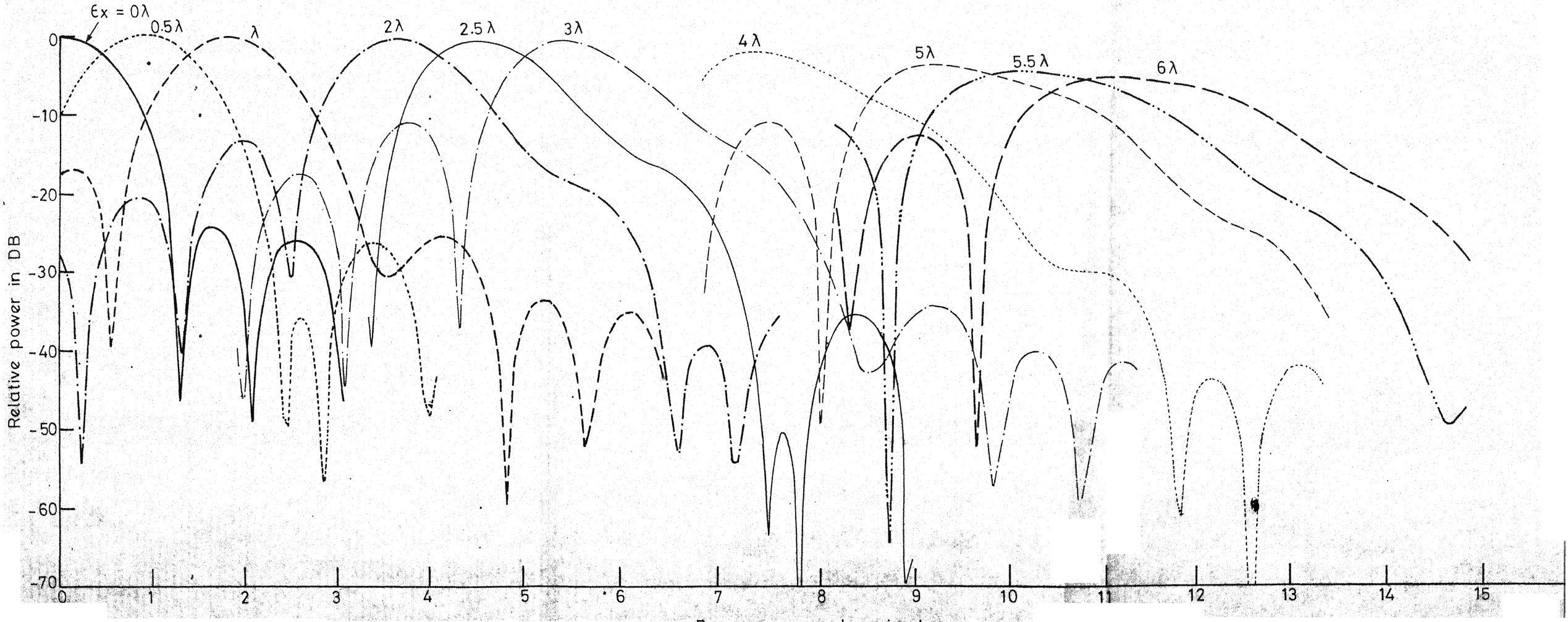

FIG. 4.5 E-PLANE PATTERN OF PARABOLID ANTENNA WITH LATERAL FEED DISPLACEMENT.

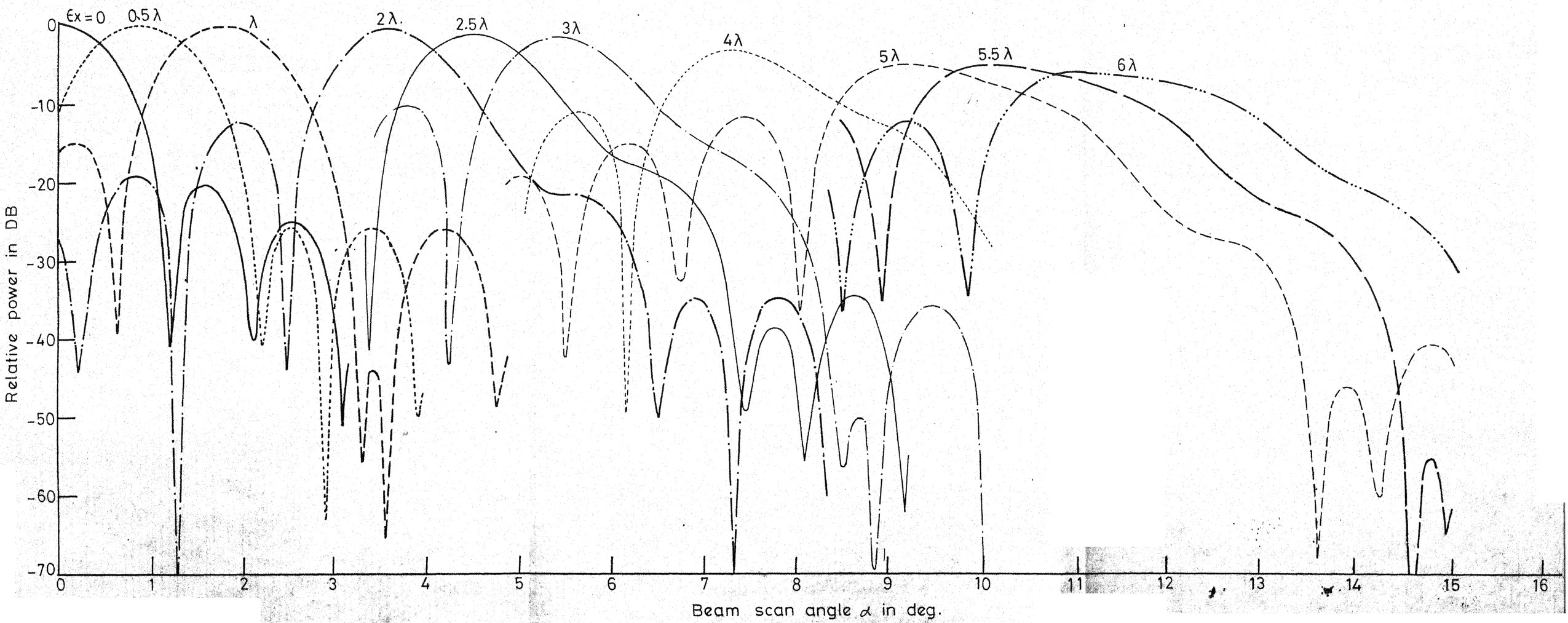

FIG. 4.6 H-PLANE PATTERN OF PARABOLID ANTENNA WITH LATERAL FEED DISPLACEMENT

For a feed displacement of one wave length in our case, this ratio is calculated to be

$$\frac{\text{Astigmatism}}{\text{Total coma}} = 0.0189$$

which is justifiably neglected for ease of computational effort.

4.3 Astigmatism in Parabolic Reflector Antennas

In chapter three, we have discussed the various causes of astigmatism in parabolic reflectors. The effect of displacement of feed is only marginal but imperfections in the reflector cause serious phase error. No reflector can be manufactured without error. Also gravitational sag changes shape of reflector surface and changes the equiphase front.

4.3.1 Astigmatism due to imperfection in surface [5]:

When the surface is imperfect, the surface of constant phase will deviate from the aperture plane, say by an amount $Z_r(x, z)$, which may be expanded as a power series [5]

$$Z_r(x, z) = \sum_{n=0}^{\infty} \sum_{m=0}^{\infty} a_{nm} \frac{x^n z^m}{(D/2)^{m+n}} \qquad (4.22)$$

where, x and z are cartisian coordinates in aperture plane y=0. If we add in this the error due to displacement of feed, say $Z_f(x,z)$, then total phase error will be

$$\varphi(x,z) = \frac{2\pi}{\lambda}(Z_r + Z_f)$$

= constant term (absolute phase) + first order term (beam shifting)

+ second order term (defocusing and astigmatism)

+ third and higher order odd terms (coma and other)

+ fourth and higher order even terms (spherical and other aber.)

We have discussed these terms neglecting astigmatism in last Sec. With astigmatism due to imperfections, second order term takes the form

$$\text{second order} = \frac{2\pi}{\lambda}\left[\frac{\alpha(z^2-x^2) + \gamma\,(z^2 + x^2)}{(D/2)^2}\right. \tag{4.23}$$

where

$$\gamma = \left[\frac{\varepsilon_z}{8}(D/f)^2 + \frac{a_{20} + a_{02}}{2}\right] \tag{4.24}$$

and

$$\alpha = \frac{a_{20} - a_{02}}{2}\text{, the astigmatism parameters} \tag{4.25}$$

Eq.(4.23) gives two second order terms: a radially symmetric error which is parabolic due to both reflector error (a_{20} and a_{02}) and axial feed position (ε_z). By setting the axial position of feed properly, this term can be reduced to zero. This feed position will maximize the peak gain of antenna and with feed in this position, the remaining second order phase error is the astigmatism term, proportional to α. Therefore, we come to the conclusion that moving the feed position for refocusing cannot eliminate astigmatism and hence proper focusing of the antenna amounts to reducing the phase error to the astigmatic form.

The effects of astigmatism can most easily be seen in the patterns of the antenna. From Eq. (4.24), it can be seen that γ varies when feed is moved axially for refocusing. This will vary the amount of phase error in each principal direction. With change in phase errors, the radiation patterns in E-plane and H-plane will vary, but differently due to the presence of astigmatism. For example when $\gamma = -\alpha$, the terms in z direction will cancel and so there will not be any phase error in the E-plane. This will provide a well formed radiation pattern with narrow beam width, small side lobes and deep nulls. Whereas in H-plane, there will be 2α parabolic error and due to this the pattern will be defocused. The effects will be a broadened main beam, high principal side lobes and poor nulls. On the other hand, when $\gamma = +\alpha$, the opposite effects will be seen. The H-plane will not have any phase error and the radiation pattern in this plane will be well formed, whereas E-plane will have a defocused pattern due to 2α parabolic error.

A compromise position of feed may provide higher gain with slight defocusing of patterns in both the planes. If the beam is elliptical astigmatism is possibly present. With astigmatism, pattern remains symmetrical, the minima fill in rapidly and the central lobe decreases in intensity along with beam broadening. Side lobes increases with the aberration, and as aberration becomes large, the main lobe no longer remains a maximum relative to the first side lobe.

4.3.2 Astigmatism in reflector due to Gravitational sag [14]:

In case of large parabolic reflectors, the reflector backing structure constitutes a weight of several tons and due to this heavy weight, the gravitational sag tends to produce a deformation such as squeezing the reflector at opposite edges in vertical plane. This would make opposite sides to move near the focus while the other two quadrant will move further away as the reflector acts like a shell. The phase in aperture plane leads in opposite quadrants and lags in the orthogonal quadrants. If the surface at a point (r, φ') is raised by $\delta n(r, \varphi')$, as shown in Figure 4.7, the wave front on the focal plane at the point r, φ' will advance by, [18]

$$\cdot\varphi = \frac{2\pi}{\lambda} 2\, \delta n(r, \varphi') \cos\left(\frac{\psi}{2}\right) \qquad (4.26)$$

Assuring, as in our earlier analysis that magnitude of aperture illumination remain unchanged, we will obtain the function $\delta n(r,\varphi')$. It is best to assume the deformation in structure of sinusoidal in nature which will provide a sinusoidal phase front. Fitting maxima and minima to the observed pattern may be done by adjusting the sine term. Bachynski [1] has tried with different sine terms and found that altering it from $\sin \frac{5\pi}{2} r$ through $\sin 2\pi r$ to $\sin \pi r$ moves the maxima and minima inwards and increases them slightly, the best fit with the observed side lobes coming with $\sin \frac{3\pi}{2} r$, where r is the normalized distance of the point r,φ' from central axis. With $\sin \frac{3\pi}{2} r$ terms, the phase front of aperture is shown in

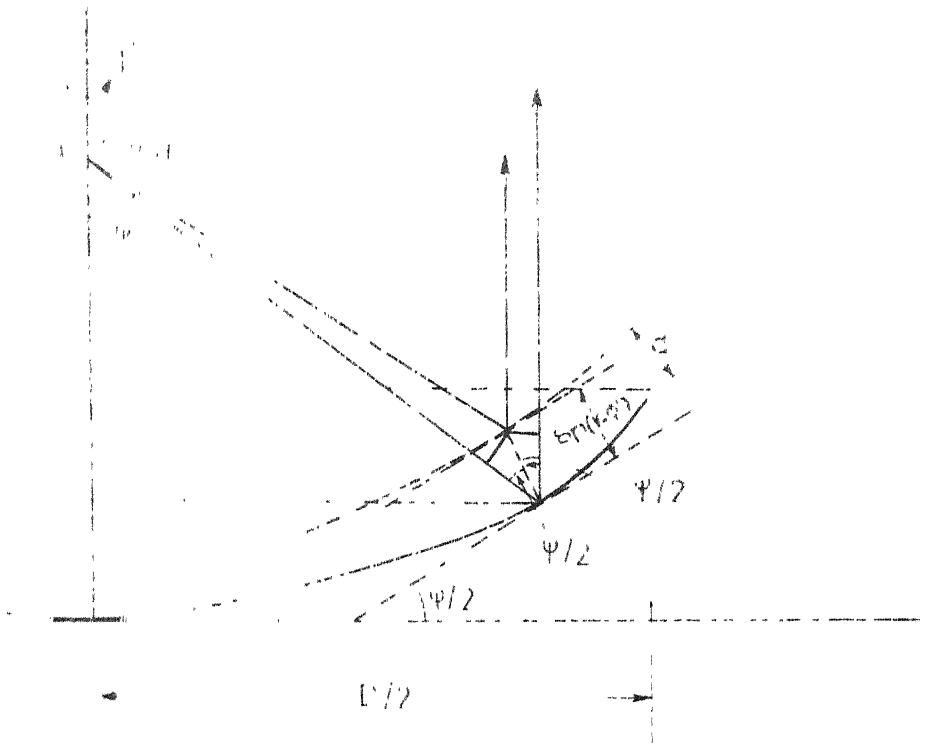

FIG. 4.7 PARABOLOID WITH ASTIGMATISM

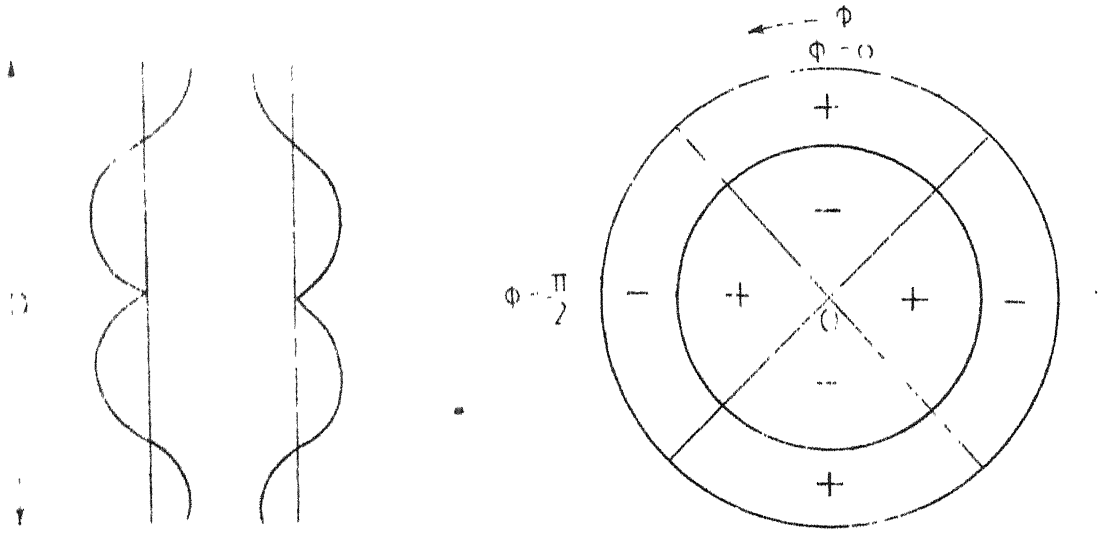

(a) $\Phi = 0$ E-plane

(b) $\Phi = \pi/2$ H-plane

(c) Reflector aperture phase with astigmatism

FIG. 4.8 APERTURE PHASE WITH ASTIGMATISM

Figure 4.8. With d as the deviation at edge of paraboloid, the function $\delta n(r, \varphi')$ is given as

$$\delta n(r, \varphi') = d \sin(\frac{3\pi}{2} r) \tag{4.27}$$

and the phase factor error becomes,

$$\Delta\varphi = \frac{2\pi}{\lambda} [2d \sin(\frac{3\pi}{2} r) \cos \frac{\psi}{2}] \tag{4.28}$$

with this phase error factor, the field integrals of Eq.(2.35) are modified as

$$E'_{ER} = \int_{-D/2}^{+D/2} f_E(z) \cos [K(z \sin \alpha + 2d \sin(\frac{3\pi}{2} r) \cos \frac{\psi}{2}] \tag{4.29a}$$

$$E'_{Ei} = \int_{-D/2}^{+D/2} f_E(z) \sin[K(z \sin \alpha + 2d \sin(\frac{3\pi}{2} r)\cos \frac{\psi}{2})] dz \tag{4.29b}$$

$$E'_{HR} = \int_{-D/2}^{+D/2} f_H(y) \cos[K(y\sin\alpha - 2d \sin(\frac{3\pi}{2} r)\cos \frac{\psi}{2})] dy \tag{4.29c}$$

and

$$E'_{Hi} = \int_{-D/2}^{+D/2} f_H(y) \sin[K(y \sin \alpha - 2d \sin(\frac{3\pi}{2}r)\cos \frac{\psi}{2})]dy \tag{4.29d}$$

The integrals are evaluated and power patterns for different deviation at edge of the dish are plotted in Figure 4.9 and 4.10 for E-plane and H-plane respectively.

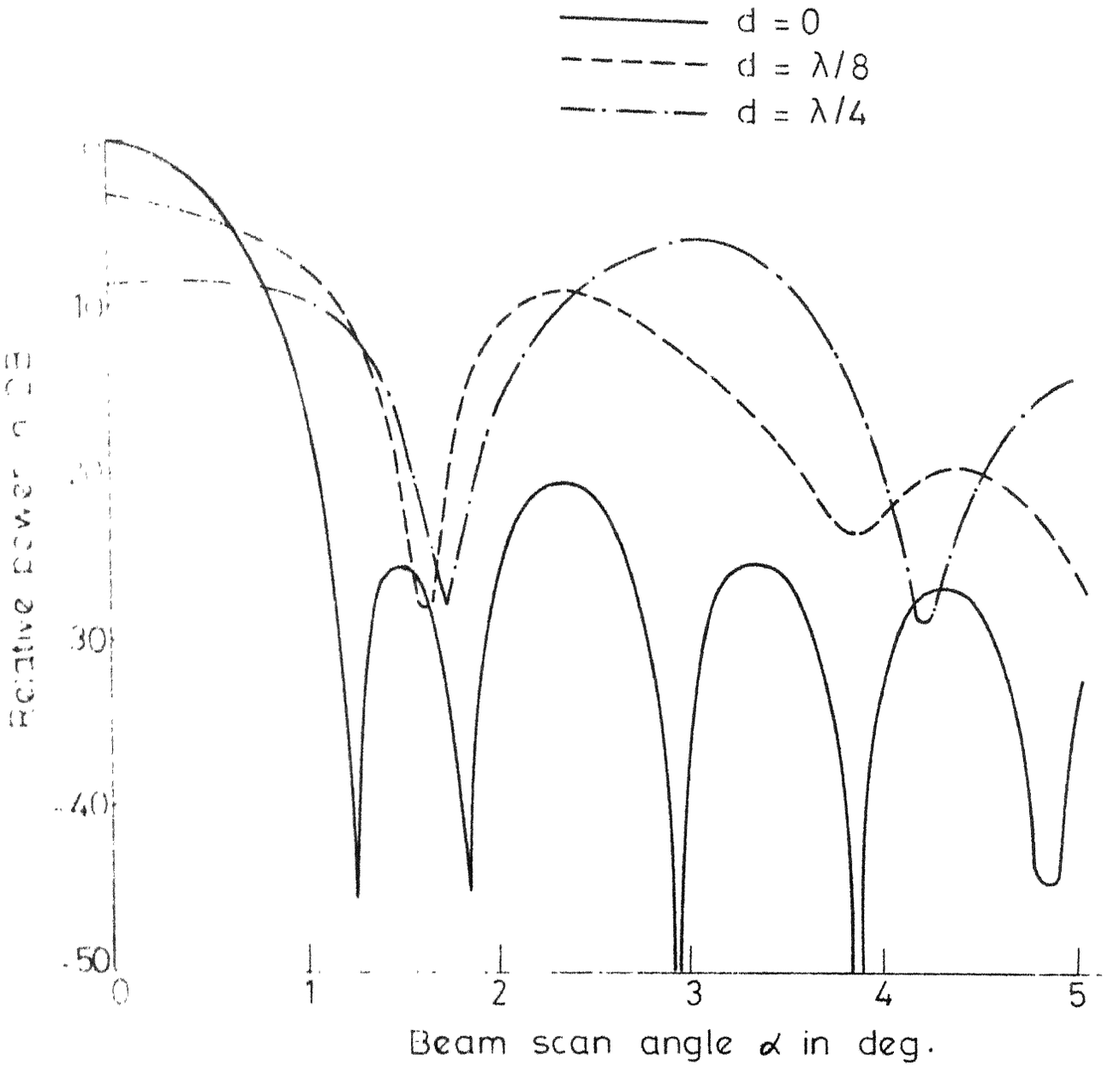

FIG 4.9a E-PLANE PATTERN OF PARABOLOID ANTENNA WITH ASTIGMATISM DUE TO GRAVITATIONAL SAG.

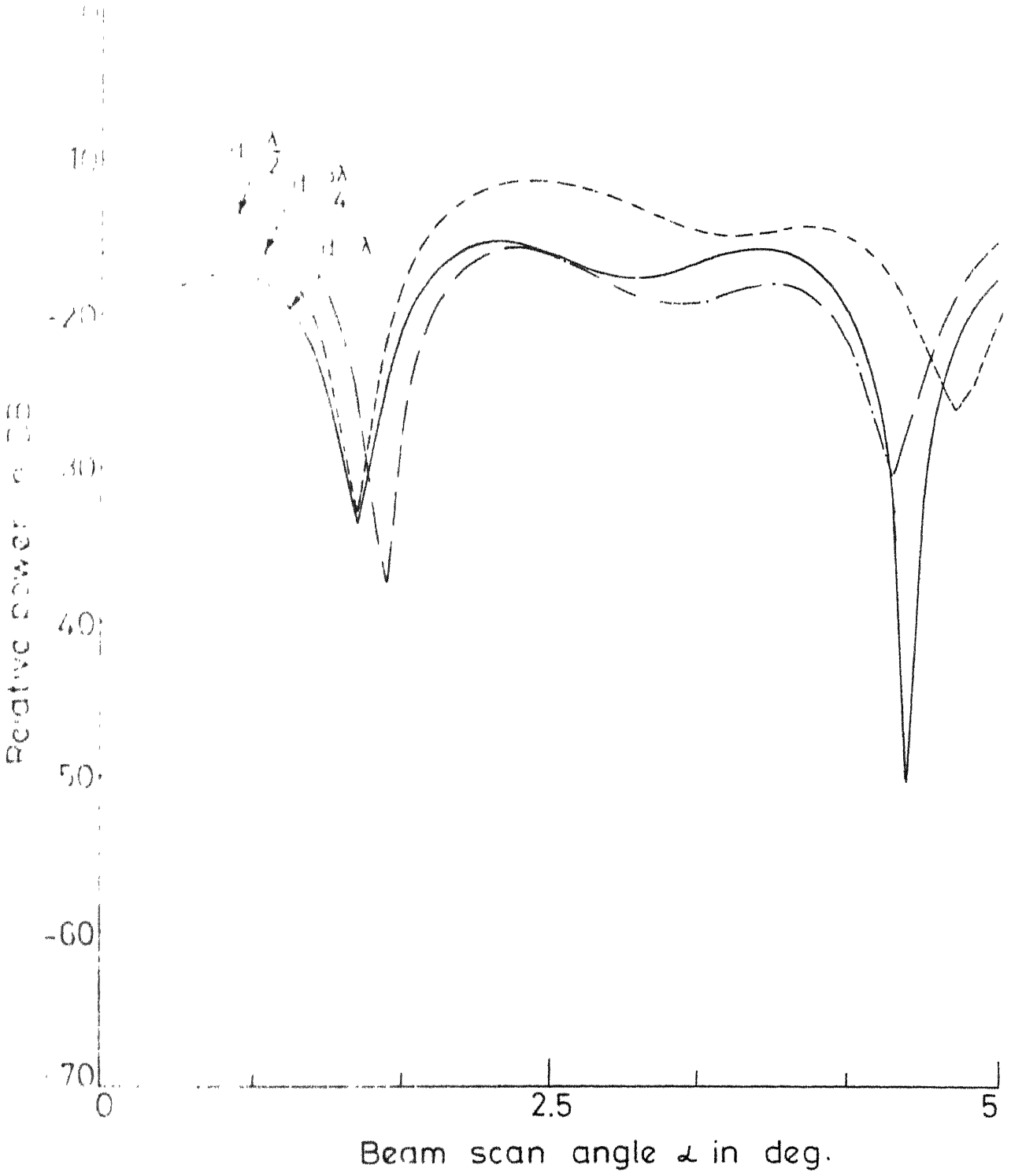

FIG 4.9b E-PLANE WITH ASTIGMATISM

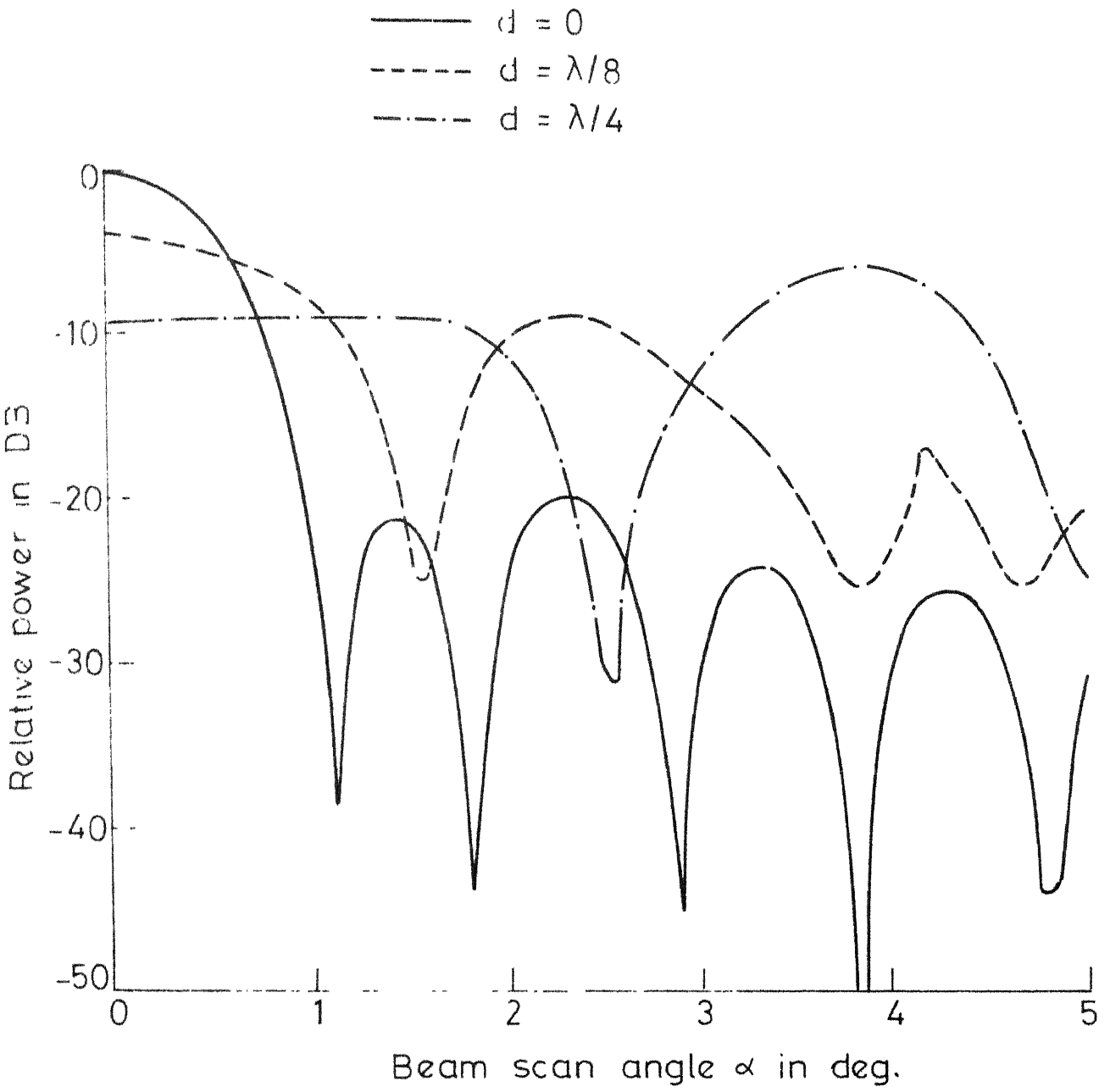

FIG. 4.10 a H-PLANE PATTERN OF PARABOLIC ANTENNA WITH ASTIGMATISM DUE TO GRAVITATIONAL SAG.

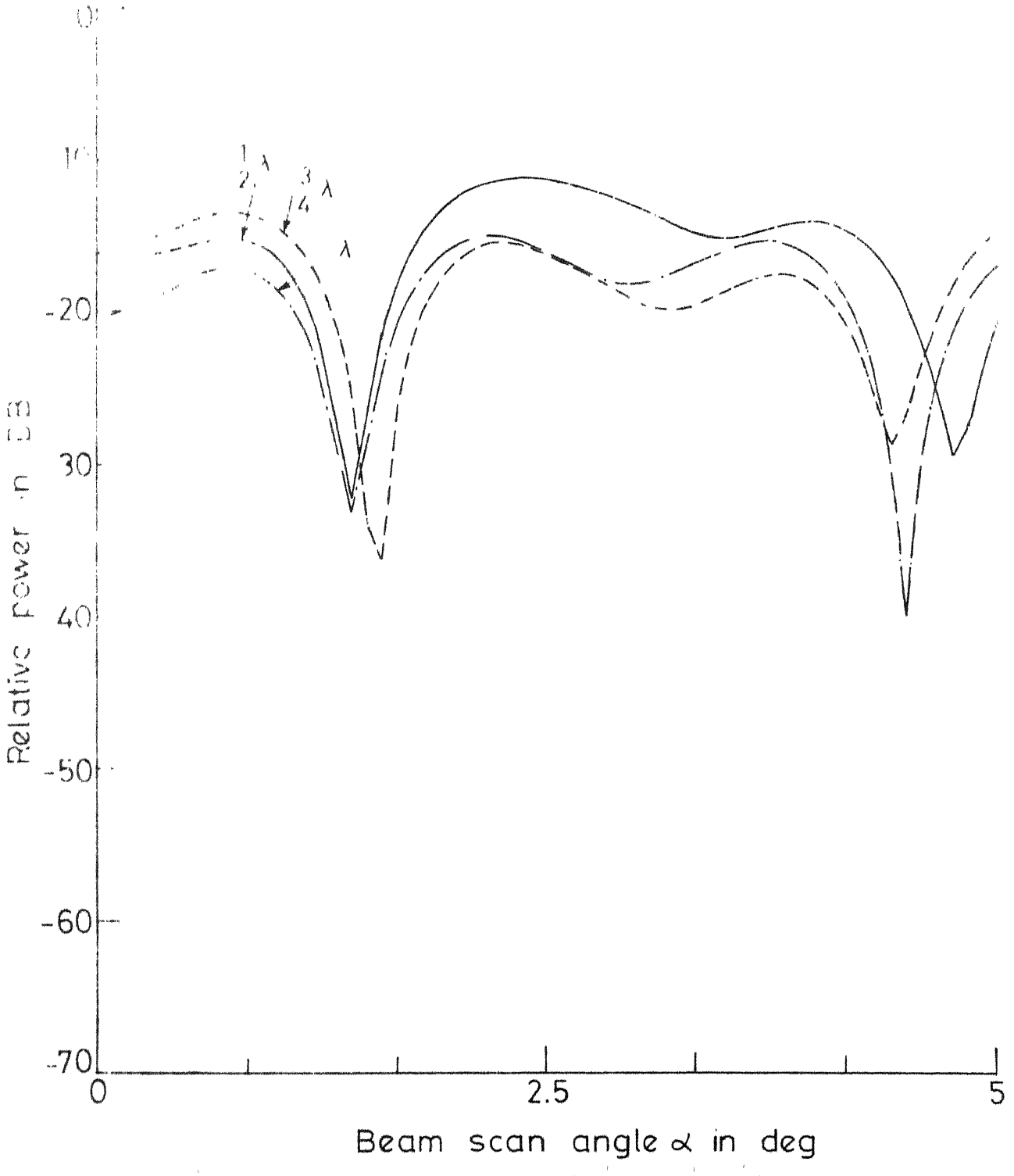

FIG. 4.10b H-PLANE WITH ASTIGMATISM

CHAPTER V

MEASUREMENT OF ANTENNA RADIATION PATTERNS

5.1 Antenna Pattern Measurement by Ordinary Methods

In order to verify the theoretical results computed earlier, an attempt was made to make pattern measurements of a parabolic reflector antenna and to study the effects of feed displacement. Existing facilities do not permit measurements on the 28 ft paraboloid for which the calculations have been made. Some experiments were attempted at the measurement of radiation patterns by ordinary methods in X-band at 10 GHz on an existing paraboloid dish with f/D ratio of 1/3, and aperture diameter of 30 cm.

The E-plane and H-plane patterns of this parabolic reflector with an E-plane sectorial horn (2.3 cm x 2.0 cm) were first computed for displacement of feed in a similar manner as done for the 28 ft dish in Chapter IV. In the experiment, the paraboloid dish was used as transmitting antenna and a pyramidal horn was used as a receiving antenna. The following factors must be taken into account while setting up the experiment.

(i) Distance between the transmitting and receiving antenna should be sufficiently large. The accepted value of the minimum distance at which pattern measurement may properly be made is $2D^2/\lambda$.

(ii) All stray reflections should be avoided since they add in a random fashion and distort the pattern. So the site for experiment should be as open as possible.

(iii) The transmitter and receiver should be kept at a sufficient height to avoid ground reflections. Their axis must also be aligned.

The measured radiation patterns in E-plane and H-plane by adjusting the feed position such as to provide maximum gain in each case, are plotted in Figure 5.1 and Figure 5.2 respectively, which are showing computed curves of radiation patterns with displacement of feed on boresight. The half power beamwidths obtained by computation and by measurements are in close agreement, whereas the radiation patterns differ widely. The reasons for disagreement may be summarized as

(i) Theoretical focal length of dish is 10 cm, whereas the best feed position was obtained when feed was approximately 11.5 cm away from the vertex.

(ii) Difference in the alignment of the axis of the parabolic reflector and receiving antenna.

(iii) Reflections from the ground and surrounding metallic objects in the laboratory could not be avoided.

(iv) The slight tilt on one side of reflector dish due to weight of the feed horn assembly.

The parabolic dish is not mounted rigidly on the rotating frame. The existing clamp arrangement for holding the feed assembly does not provide steady and accurate

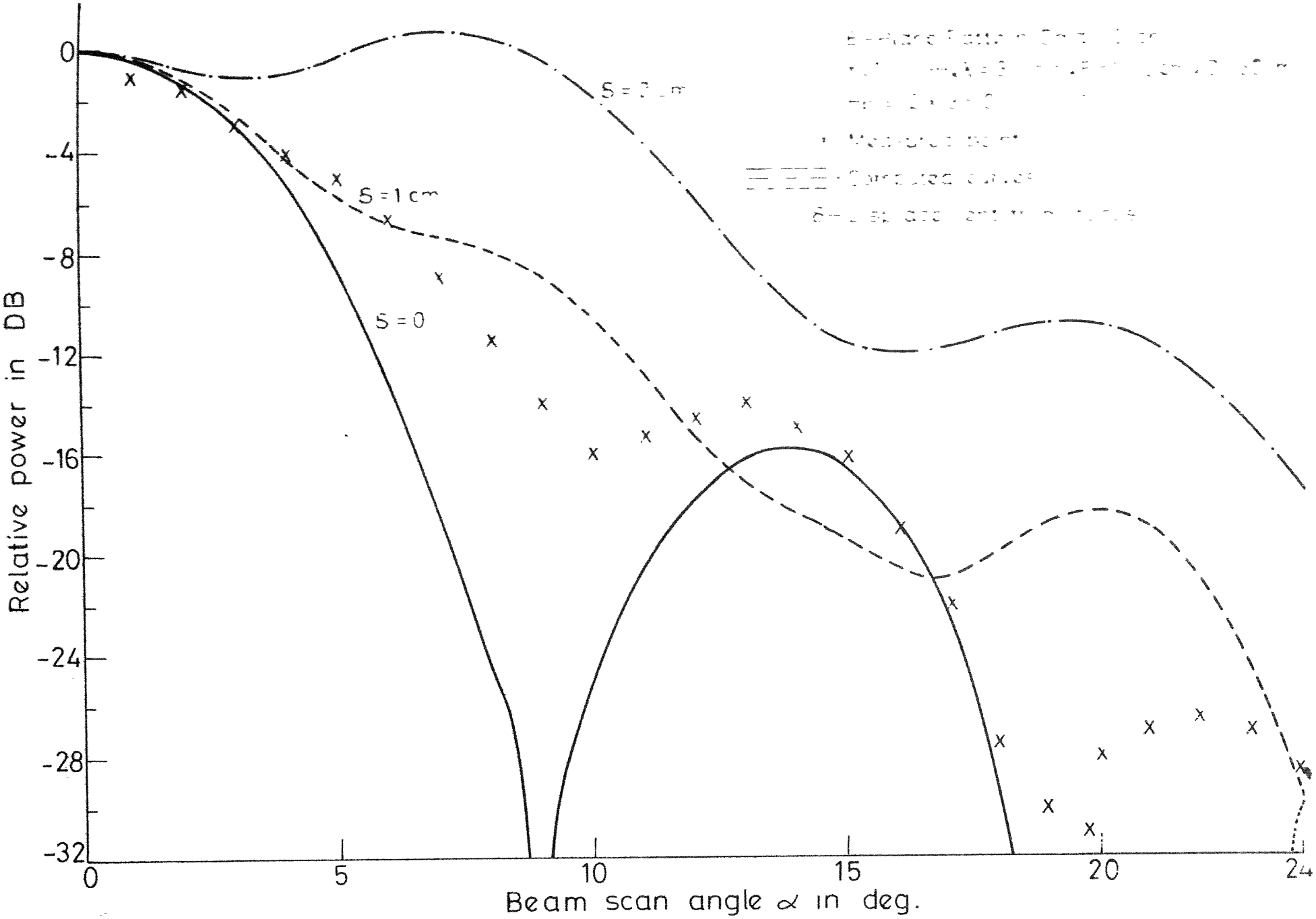

FIG.5.1 E-PLANE RADIATIONAL PATTERN OF PARABOLOID IN X BAND

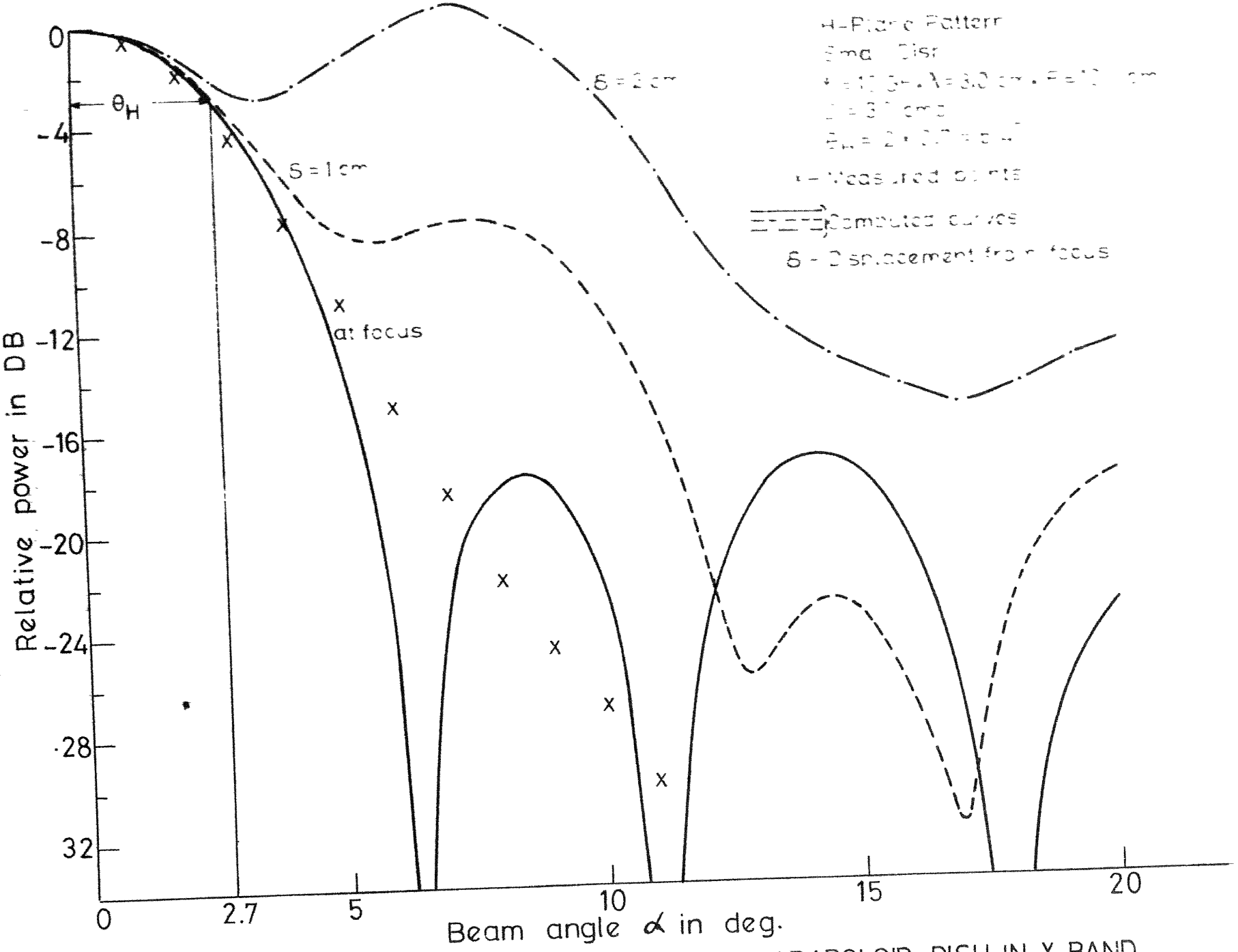

FIG. 5.2 H-PLANE RADIATION PATTERN OF PARABOLOID DISH IN X BAND

movement of feed horn. There is no mechanism available, which can be attached to the frame of the dish by which the feed can be moved from one position to another desired position. In the existing system, once the feed is moved from one location, it is very difficult to ascertain its movement on the same axis or in a particular plane. All this has to be done by personal judgement alone, which results in errors in the measurement.

The measured values of field strength at various positioning of the feed are, therefore at variance with the ones computed, and hence are not plotted on the graphs. The two most essential requirements which must be complied, if the existing parabolic dish is to be used for antenna measurement with displacement of feed from the focus are -

(i) Proper aligning and firmly mounting the parabolic dish on the rotating frame.

(ii) Designing and fabricating a mechanism to facilitate accurate measurement of distance from the vertex to feed and also to permit movement of feed in desired plane or axis.

Lastly, the experiment should be conducted in an open place to avoid stray reflections.

The ordinary method of antenna pattern measurement cannot be used with very large parabolic reflectors. The main limitation comes from the requirement of distance, that is needed between the transmitting source and the receiving

source for good pattern measurement. It is known to us that this distance should not be less than $2D^2/\lambda$. To feel the magnitude, let us consider the troposcatter dish with 28 ft (8.5 m) aperture diameter operating at 2.1 GHz (λ=14.286 cm). The distance needed will be approximately 1 Km, which is a very large distance. Different methods will have to be used to obtain radiation pattern in such cases.

5.2 Measurement of Antenna Radiation Patterns of Large Parabolic Reflectors

We have calculated above that distance needed between the two sources, when one of them is a large parabolic reflector dish is very large for obtaining good radiation pattern. One way to measure radiation pattern at such a large distance is by using parabolic reflector dish as a transmitting source and placing a receiving source in an aircraft. Now, by arranging the flight of aircraft in one of the plane in the radiation zone and obtaining the cross-section of the transmitting lobe, radiation pattern can be built up by plotting the cross-section of lobe at varying distances from the transmitter, i.e., parabolic reflector dish. The other method is to use the parabolic reflector antenna as a receiving source and natural transmitters as the far field source. These natural transmitters are the extra-terrestrial sources of radio emission.

The two methods mentioned above will now be discussed in some detail.

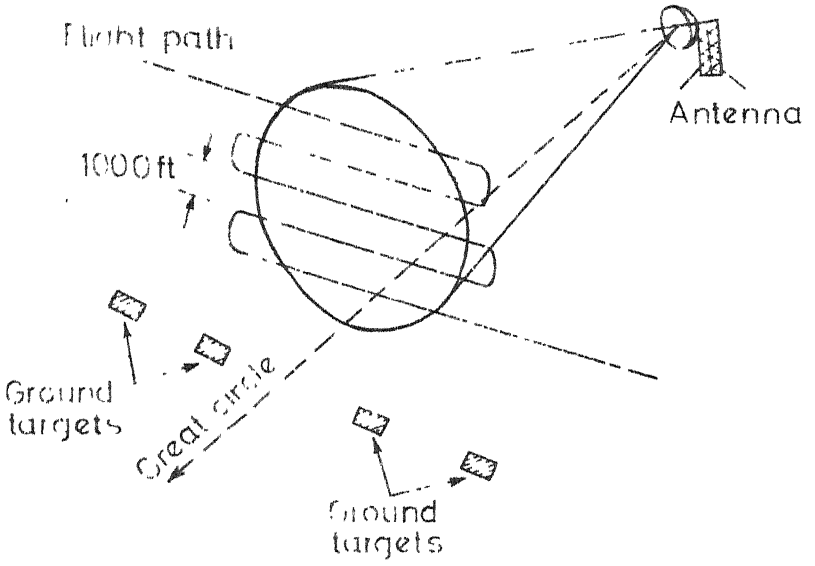

FIG. 5.3 FLIGHT PATTERN FOR MEASURING CROSS-SECTIONS OF THE ANTENNA BEAMS.

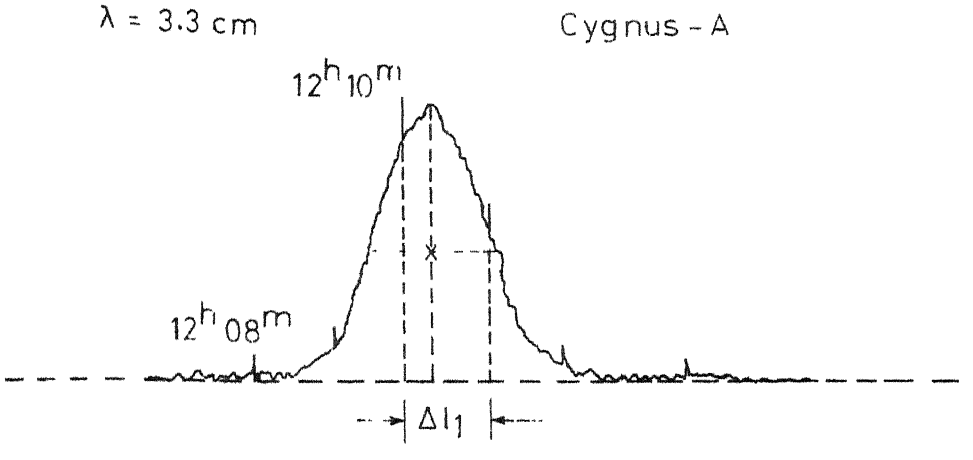

FIG. 5.4 AN EXAMPLE OF A RECORDING OF THE DRAFT CURVE OF A SOURCE CYGNUS-A THROUGH AN ANTENNA'S DIRECTIONAL PATTERN. Δl_1 IS THE DISTANCE BETWEEN MINUTE TIME MARKINGS.

5.2.1 Measurement of Radiation Pattern with the Aid of Aircraft [2]

A schematic representation of the flight pattern to obtain the cross-section of radiation pattern at one plane is shown in Figure 5.3. To obtain the beam cross-section at various places, number of flights are to be flown at each plane. Level flights at altitude intervals of 1000 ft. are to be flown well beyond each side of the major lobe of the ground antenna. Flights should maintain a level to the accuracy of ±50 ft. The flight track can be controlled by use of a gyrostabilized drift sight over a course of ground targets which should be carefully surveyed in position and direction. To permit interpolation of position between the targets, exact time of passage over the target must be recorded.

A downward looking camera or telescope may be used for correct identification of targets. Precaution should be taken to plan flights in a cloud free and stable weather. This will facilitate easier operation and give better results. Once the cross-sections of lobe at different distances from antenna are known, the radiation pattern can be built up. To obtain high accuracy, it is necessary to determine precisely the coordinates of the aircraft in flight, as well as to maintain high stability. This along with the economic factors involved make the use of this method exceedingly difficult.

5.2.2 Measurement of Radiation Pattern with the aid of Extraterrestrial Sources of Radio-emission [12]:

The increasing knowledge of extraterrestrial sources in the field of 'Radio-astronomy' have made it possible to make use of the socalled 'radio stars' which emit in addition to visible light, electromagnetic radiation. This emission of radio waves is filtered by atmosphere and available in wavelength from 1 mm to 15-20 m. The main characteristic features of this radio emission are that this signal is very weak and it has a noise character similar to the internal noise of radio receivers and amplifiers; i.e. uniform with Gaussian distribution over the bandwidth of receiving system. Therefore, a very sensitive, superhetrodyne receiver should be used for receiving this weak signal, and arrangement made for recording an incremental increase in output from constant level that is due to internal noise. This device is usually called Radiometer.

The measurement of antenna's directional pattern using such source consists of the recording of the transit curves from the source and subsequent analysis of this curve. Before antenna pattern measurements can be made, it is necessary to align the antenna's electrical axis with geometrical axis, the direction where the paraboloid's directional pattern is maximum. This is also achieved by recording of the transit curves. Steps taken to obtain the recording of these drift curves are:

i) Select an appropriate extraterrestrial source and calculate the local time of culmination on the day intended for measurement.

ii) Put geometrical axis in the meridian plane as trajectories are horizontal at the culmination point.

iii) Obtain the azimuth angle A and elevation angle h of point source from the equiatorial coordinates by using transformation equations.

iv) Warm the recording device long enough so that zero level and amplification are stabilized, and start recording well ahead of the measurement time to ensure a reliable measurement of the zero level.

If the calculations are correct and the displacement between the electrical and geometrical axes is not too large, the emission source 'enters' the antenna directional pattern before culmination, crosses the pattern and then 'leaves'. Figure 5.4 shows such a recording from source Cygnus-A. If large fluctuations are observed on the recording, several curves must be averaged. Several recordings of drift curves should be made of a source's passage near culmination with both positive and negative deviation in elevation angle h. Recording with maximum amplitude will give the correct alignment of electrical axis.

When emission is from a point source, the recording of a source's transit across the antenna with electrical axis aligned reproduces the directional pattern, say $F(\theta)$. But when

the source's angular dimensions are large compared to the antenna's main beam (normally beamwidth at half power point) e.g. the sun, then this leads to broadening of the recorded curve. However, in most cases, the broadening of the directional pattern can be compensated for when the recordings are analyzed. Let $F_f(\theta)$ be the pattern obtained from the transit of such source with finite dimension R, the angular radius of constant brightness temperature portion of the dish source. Then relationship between $F(\theta)$ and $F_f(\theta)$ developed by Boguslavtsev is given as

$$F(\theta) = [F_f(\theta) + \frac{R^2}{8} F_f''(\theta) + \frac{R^4}{192} F_f''''(\theta) + \ldots] \qquad (5.1)$$

Thus the function $F(\theta)$ can be represented by a converging series. When

$$\frac{R^2}{8} F_f''(\theta) << F_f(\theta) \qquad (5.2)$$

the curve $F_f(\theta)$ obtained from the source's passage is similar to $F(\theta)$, the directional pattern obtained from a point source.

CHAPTER VI

RESULTS AND DISCUSSIONS

6.1 Summary of Results and Discussion

6.1.1 Defocusing:

Information obtained from the curves for radiation pattern of parabolic reflector antenna with displacement of feed on borcsight shown in Figures 4.2 and 4.3 are given in Table 6.1.

It can be seen from the data obtained as well as from the curves that as the feed displacement increases, there is a reduction in field intensity, increase in half power bandwidth and blending of the side lobes into the main beam. The level of second side lobe decreases with increase in displacement of feed, whereas the levels of subsequent side lobes do not change appreciably. The gain of antenna falls rapidly when feed displacement increases more then 3/4th wavelength.

6.1.2 Off-set feed:

Results for off-set feed from curves drawn in Figure 4.5 and Figure 4.6 are tabulated in Table 6.2. It can be seen from the diagrams that as the feed displacement increases, the beam shift also increases, coupled with reduction in field intensity and increase in beamwidth. The beam no longer remains symmetrical, which is the effect of comatic aberration. It can be observed that the level of

TABLE 6.1: CHARACTERISTIC OF PARABOLOID ANTENNA WITH FEED DISPLACEMENT ON BORESIGHT

Displacement of feed from boresight in wavelength	Reduction in field intensity (db)		First side lobe level (db)		Second side lobe level(db)		Third side lobe level (db)		Half power beamwidth in deg.		Gain (db)
	E	H	E	H	E	H	E	H	E	H	
0	-	-	-25.5	-21.25	-20.62	-19.90	-25.5	-24.16	0.96	0.94	44.8
1/4	0.251	0.258	X	X	-22.10	-21.11	-24.4	-23.70	0.98	0.96	44.6
1/2	1.024	1.054	X	X	-26.64	-24.13	-24.0	-23.06	1.10	1.00	43.9
3/4	2.376	2.457	X	X	X	X	-24.16	-23.35	1.30	1.20	42.4
1	4.420	4.608	X	X	X	X	-26.70	-25.53	3.05	3.02	34.7

Note: X means the side lobe in submerged in the main lobe.

TABLE 6.2: CHARACTERISTIC OF PARABOLOID ANTENNA WITH OFF-SET FEED

Displacement of feed in transverse plane in wavelength	Reduction in field intensity (db)		Beam tilt in deg.		Beam deviation factor BDF		Half power beamwidth in deg.		Gain in (db)	Efficiency of antenna (percent)
	E	H	E	H	E	H	E	H		
0.0	-	-	-	-	-	-	1.03	1.01	44.2	100.0
0.5	0.04	0.04	0.91	0.91	0.834	0.834	1.04	1.02	44.1	99.1
1.0	0.16	0.17	1.83	1.83	0.834	0.834	1.06	1.03	43.9	96.4
2.0	0.63	0.63	3.57	3.57	0.815	0.815	1.09	1.04	43.8	85.8
2.5	0.98	0.99	4.48	4.48	0.819	0.819	1.13	1.06	43.5	79.5
3.0	1.42	1.44	5.40	5.40	0.822	0.822	1.16	1.11	43.2	72.0
4.0	2.54	2.58	7.23	7.23	0.824	0.824	1.29	1.20	42.4	55.7
5.0	3.96	4.07	9.14	9.05	0.834	0.826	1.70	1.47	40.3	39.8
5.5	4.76	4.95	10.13	9.97	0.842	0.826	2.00	1.83	38.7	33.5
6.0	5.53	5.87	11.29	11.05	0.857	0.840	2.20	2.13	37.6	28.0

side lobe towards the boresight is higher whereas on the other side of main lobe it is much lower. The beam broadens at base away from boresight so that the side lobes merge with the main beam. The deformation of beam for an off-set feed of more than one wavelength restricts the beam scan to approximately ± 2 SBW without much degradation.

6.1.3 Astigmatism :

It can be seen from curve of Figure 4.9 and Figure 4.10 that the astigmatic aberration due to imperfection in structure when gravitational sag deforms the reflector surface, causes rapid degradation of radiation pattern. Table 6.3 provides the information about the reduction in field intensity, first side lobe level and half power beamwidths, for various values of deviation in reflector surface at edge of the dish. There is sharp reduction in field intensity, increase in side lobe level and beam broadening with increasing value of deviation. With deviation more than 1/8th wavelength, the main lobe no longer remains a maxima relative to side lobe level.

6.2 Conclusions

We have studied the effects of various aberrations on radiation pattern of a parabolic reflector antenna, which are caused by displacement of feed from its focus and departure of reflector surface from true paraboloid. Displacement of feed on boresight causes defocusing of radiation pattern by increasing its half power beamwidth, blending side lobes into main beam and bringing a reduction in field intensity. Such a displacement of more than half wavelength degrades the

TABLE 6.3: CHARACTERISTIC OF PARABOLOID ANTENNA WITH ASTIGMATISM

Deviation at edge of reflector dish in wavelength	Reduction in field intensity (db)		First side lobe level (db)		Half power beamwidth in deg.	
	E	H	E	H	E	H
0			-25.60	-21.10	0.96	0.94
1/8	3.58	3.85	- 8.98	- 8.70	2.00	2.00
1/4	8.70	9.22	- 5.99	- 5.96	2.45	2.41
1/2	16.08	16.66	-10.61	-10.74	2.16	2.35
3/4	15.32	16.21	-15.10	-15.00	2.30	2.61
1	19.52	20.39	-14.56	-14.60	2.28	2.28

radiation pattern severely and reduces the antenna gain. Therefore, feed should be positioned very carefully and as close as possible to the focus to avoid any loss of directivity and reduction in resolution.

The effects of astigmatism on parabolic reflector antenna due to imperfection or deviation of reflector surface from true paraboloid is also quite severe. The surface of the parabolic reflector must be manufactured to a high precision It is difficult to manufacture an absolutely perfect paraboloidal surface, so a small amount of astigmatic aberration is always present. Greater precautions should be taken to counter gravitational stresses while designing the back structure so that surface is kept to a near perfect paraboloid.

The displacement of feed on transverse axis causes a tilt in the main beam and provides the possibility to achieve a beam scan. However, along with linear phase shift, cubic phase error brings comatic aberration, which degrades the radiation pattern by blending the side lobes away from boresight into main beam, increasing side lobe level towards boresight and causing an opposite shift of main beam. The shift in reverse direction reduces the beam tilt to a value less than feed squint, thus bringing beam deviation factor into picture. Degrading of radiation pattern due to astigmatism and defocusing in off-set feed case is negligible compared to coma and so it is comatic aberration which put restrain on the range of beam scanning. A beam scanning of about ± 2 SBW can be achieved by keeping the efficiency of system above 90 percent.

APPENDIX 'A'

```
C     PROGRAM FOR EVALUATING E-PLANE PATTERN OF AN OFF AXIS HORN
C     FEED PARABOLOID
C     ***********************************************************
C     THE INTEGRAL INVOLVED IN EXPRESSION FOR RADIATION PATTERN IS
C     DENOTED BY F(X) AND IS EVALUATED USING
C     'V' APPLICATION OF SIMPSON'S RULE BETWEEN INTEGRATION
C     LIMITS A AND B. SUMND IS THE SUM OF ALL F(X(I)) FOR EVEN
C     I(EXCEPT FOR F(X(2*N))) WHILE SUMID IS THE SUM OF ALL
C     F(X(I)) FOR ODD.
C     ***********************************************************
      DIMENSION VA(100)
      DIMENSION FACT(250)
      COMMON/DATPI,ALMDA,FL,ALPA,DELTA
      COMMON/BSL/FACT
      REAL JO
      CALL FLUN(31000)
C     ALMDA-WAVELENGTH IN CM
C     SMALB-E-PLANE APERTURE OF THE HORN IN TERMS OF WAVELENGTH
C     DIAMTR-DIAMETER OF PARABOLIC REFLECTOR IN TERMS OF WAVELENGTH
C     FLNT-FOCAL LENGTH OF PARABOLOID IN WAVELENGTHS
      ALMDA=14.286/14.286
      PI=4.*ATAN(1.)
      DIAMTR=28.*.305/.14286
      SMALB=11./14.286
      FLNT=12.4*.305/.14286
      FL=.305*(12.4-3.95)/.14286
      A=0.305*14.0/.14286
      FACT(1)=1.
      DO 200 KK=2,30
      KKK=KK-1
200   FACT(KK)=FLOAT(KK)*FACT(KKK)
      DELTA=0.0
C     DELTA-DISPLACEMENT OF FEED IN WAVELENGTHS
11    PRINT 75,DELTA
75    FORMAT(20X,E15.8)
      DELTA=DELTA/FLNT
      KI=0
      DO95 IK=401,801,5
      IF(DELTA*FLNT-3.)12,12,13
12    PIK=IK-401
      GO TO 14
13    PIK=IK-1
14    ZIK=PIK*PI/180.
      ALPA=ZIK*ALMDA/DIAMTR
      KI=KI+1
C     N IS NO OF INTERVALS BETWEEN INTEGRATION
      N=50
      AN=N
```

```
      STEP = 1.0/AN
      H=STEP/2.
C     INITIALISE PARAMETER
      SUMND=0
      SUMID=0
C     FOR EACH INDIVIDUAL APPLICATION OF SIMPSON'S RULE 'I' IS
C     ITERATION COUNTER
      DO 85 I=1,N
C     EVALUATE SUMND,SUMID
      TEMP=I-1
      XX=STEP*TEMP
      IF(XX.EQ.0.) GO TO 85
      Z1=1.+(A*XX/(2.*FLNT)**2.
      A1=SIN(ALPA)-(DELTA/Z1)
      FT1=2.*PI*XX*A1/ALMDA
      FT1=A*FT1
      CALL BESL(FT1,JO)
      AI1=JO
      Z2=1.+(A*(XX+H)/(2.*FLNT))**2.
      A2=SIN(ALPA)-(DELTA/Z2)
      FT2=2.*PI*(XX+H)*A2/ALMDA
      FT2=A*FT2
      CALL BESL(FT2,JO)
      BI1=JO
      SUMND=SUMND+F(XX)*AI1
      SUMID=SUMID+F(XX+H)*BI1
85    CONTINUE
C     ESTIMATE VALUE OF THE INTEGRAL
      CI1=1.0
      Z4=1.+(A/(2.*FLNT))**2.
      A4=SIN(ALPA)-(DELTA/Z4)
      FT4=2.*PI*A*A4/ALMDA
      CALL BESL(FT4,JO)
      DI1=JO
      VALUE=(2.*SUMND+4.*SUMID-F(0.0)*CI1+F(1.0)*DI1)*H/3.
      VALUE=(VALUE*VALUE)
      IF(IK.NE.401) GO TO 90
      IF(DELTA.NE.0.) GO TO 90
      ANOR=VALUE
90    CONTINUE
C     VALUE IS NORMALISED POWER
      VALUE=VALUE/ANOR
C     VALU IS NORMALISED POWER IN DBS'
      VALU=10.*ALOG10(VALUE)
      VA(KI)=VALU
      ALPADG=180.*ALPA/PI
95    CONTINUE
      PRINT40,(VA(KI),KI=1,81)
40    FORMAT(10(3X,F8.4)
      PUNCH101,(VA(KI),KI=1,81)
101   FORMAT(10F8.4)
15    DELTA=DELTA*FLNT
16    DELTA=DELTA+1.0
```

```
      IF(DELTA-6.)17,17,18
17    GO TO 11
18    STOP
      END


C     EVALUATION OF BESSEL  FUNCTION
      SUBROUTINE BESL(X,JO)
      DIMENSION FACT(250)
      COMMON/BSL/FACT
      CALL FLUN(31000)
      REAL JO,JOO,JOX
      IF(X)10,15,10
15    JO=1.0
      RETURN
10    JO=1.0
      PI=4.0*ATAN(1.0)
      IF(X-13.0)45,45,60
45    ERSLN=1.E-20
      B=ABS(X)*0.5
      DO 50 M=1,30
      RM=M
      IF(M-(M/2)*2)35,30,35
30    MMM=1
      GO TO 40
35    MMM=-1
40    JOX=FLOAT(MMM)*((B**RM)/FACT(M))*((B**RM)/FACT(M))
      JOO=JO
      JO=JO+JOX
      CONST=JO-JOO
      IF(ABS(CONST).LE.ERSLN) GO TO 100
50    CONTINUE
100   RETURN
60    JO=SQRT(2.0/(PI*X))*COS(X-0.25*PI)
      RETURN
      END


C     EVALUATION OF FUNCTION F
      FUNCTION F(Z)
      COMMON/DAT/PI,ALMDA,FL,ALPA,DELTA
      A=0.305*14.0/.14286
      AK=2.*PI/ALMDA
      SMALB=11./14.286
      FL=.305*(12.4-3.95)/.14286
      PHIZ=ATAN(A*Z/FL)
      IF(PHIZ.EQ.0.) GO TO 10
      UE=AK*SMALB/2.*SIN(PHIZ)
      F=SIN(UE)*A*Z/UE
      RETURN
10    F=A*Z
      RETURN
      END
```

REFERENCES

1. Bachynski, M.P. and Bekefi, G.: 'Aberrations in circularly symmetric microwave lenses', IRE Trans. Ant. and Prop., Vol.4, pp.412-421, July 1956.

2. Beamer, C.M.: 'Measurement of antenna beam cross-section', Report from Collins Radio Company for a 230-km troposcatter circuit, pp.5-6.

3. Berkowitz, B.: 'Antennas fed by horns', Proc.IRE, Vol.41, pp.1761-1765, Dec.1953.

4. Blake, L.V.: 'Antennas', John Wiley, New York, pp.191-195, 1966.

5. Cogdell, J.R. and Davis, J.H.: 'Astigmatism in reflector antenna', IEEE Trans. Ant. and Prop., Vol.21, pp. 565-567, July 1973.

6. Fradin, A.J.: 'Microwave Antenna', Pergamon Press, New York, Chap.7, pp. 417-421, 1961.

7. Hansen, R.C.: 'Microwave Scanning Antenna', Vol.I, Academic Press, New York, Chap.I, pp.47-51, Chap.II, pp.139-146, 1964.

8. Ingerson, P.G. and Rush, W.V.T.: 'Radiation from a paraboloid with an axially defocussed feed', IEEE Trans. Ant. and Prop., Vol.21, pp.104-106, Jan.1973.

9. Jasik, H.: 'Antenna Engineering Handbook', McGraw-Hill Book Co., New York, 1961, pp.12-12.

10. John Ruze; 'Lateral feed displacement in a paraboloid', IEEE Trans. Ant.and Prop., Vol.13, pp.660-665, Sept.1965.

11. Kelleher, K.S.: 'Scanning antennas', in Antenna Engineering Handbook (H. Jasik), 1961, pp.15-20.

12. Kuz'min, A.P. and Salomonovich A.E.: 'Radio-astronomical methods of antenna measurement', Academic Press, New York, 1966, Chap.1, pp.10-15, Chap.4, pp.108-126.

13. Lo, Y.T.: 'On beam deviation factor of a parabolic reflector', IRE Trans. Ant. and Prop.Vol.8, pp.347-349, May 1960.

14. Miller, P: Computation of Polar diagrams from paraboloidal reflector aerials with systematic deformations', Electronic Letter (GB), Vol.4, pp. 398-400, Sept. 1968.

15. Rudge A.W. and Withere, M.J.: 'New technique for beam steering with fixed parabolic reflectors', Proc. Inst.EE (GB), Vol.118, pp.857-863, July 1971.

16. Sandler, S.S.: 'Paraboloidal reflector patterns for off axis feeds' IRE Trans., Ant. and Prop. Vol.8, pp.368-379, July 1960.

17. Silver, S.: 'Microwave Antenna theory and design', McGraw-Hill, New York, 1949, Chap.12, pp. 413-417.

18. Slater, R.H.: 'Radiation pattern of imperfect paraboloidal reflectors', Electron. Letter (FB), Vol.6, pp. 796-798, Dec.1970.

19. T. Takeshima: 'Beam Scanning of parabolic antenna by defocusing', Electron. Letter (GB), Vol.41, pp. 70-72, Jan. 1961.

20. Wheeler, H.A.: 'Antenna beam patterns which retains shape with defocusing', IRE Trans. Ant. and Prop. Vol.10, pp. 573-580, Sep.1962.

21. Wolff, E.A.: 'Antenna Analysis', John Wiley and Sons, New York, 1966, Chap.4, pp.119-127; Chap.7, pp.313-323.

ADDITIONAL REFERENCES

1. Born, M. and Wolff, E.: 'Principles of Optics', Pergamon Press, New York, 1959.

2. Kraus, J.D.: 'Antennas' , McGraw-Hill, New York, 1950.

3. Rush W.V.T. and Potter, P.D.: 'Analysis of reflector antennas', Academic Press, New York, 1970.